

9-2018

Design of Wind Turbine Tower Height and Blade Length: an Optimization Approach

Ryan Wass

Follow this and additional works at: <http://scholarworks.uark.edu/meeguht>



Part of the [Energy Systems Commons](#)

Recommended Citation

Wass, Ryan, "Design of Wind Turbine Tower Height and Blade Length: an Optimization Approach" (2018). *Mechanical Engineering Undergraduate Honors Theses*. 70.
<http://scholarworks.uark.edu/meeguht/70>

This Thesis is brought to you for free and open access by the Mechanical Engineering at ScholarWorks@UARK. It has been accepted for inclusion in Mechanical Engineering Undergraduate Honors Theses by an authorized administrator of ScholarWorks@UARK. For more information, please contact scholar@uark.edu, ccmiddle@uark.edu.

DESIGN OF WIND TURBINE TOWER HEIGHT AND BLADE LENGTH: AN OPTIMIZATION APPROACH

A HONOR THESIS SUBMITTED IN PARTIAL
FULFILLMENT OF THE REQUIREMENTS FOR THE
HONOR STUDIES IN MECHANICAL ENGINEERING

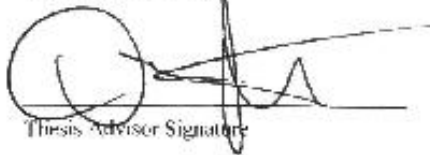
by

Ryan Wass

University of Arkansas
Bachelor of Science in Mechanical Engineering
April 2018

Darin Nutter

Thesis Advisor Name



Thesis Advisor Signature

LARRY ROE

First Committee Member Name



First Committee Member Signature

ACKNOWLEDGEMENTS

I would first like to thank Dr. Darin Nutter for giving me the opportunity to pursue this research. I am grateful for the guidance and support that Dr. Nutter has provided me throughout this experience. With a little push from him I was able to dive into the renewable energy industry and have gained valuable experience during this research. Thank you for allowing me to study more about my passion.

I would also like to thank my friends and family for their support through the long nights and early mornings. Thank you for always knowing where the comma should go.

ABSTRACT

The wind industry is a fast growing market and is quickly becoming competitive with traditional non-renewable energy resources. As with any developing industry, research must continually be redefined as more complex understandings of design variables are learned. Optimization studies are common ways to quickly refine design variable selections. Historical wind turbine data shows that the tower hub height to rotor diameter ratio scales almost linearly. However there is no specific rule that dictates the optimum hub height for a given diameter. This study addresses this question by using an Excel based optimization program to determine the height to diameter ratio of a simulated turbine with the lowest cost of energy. Using a wind turbine power curve database and previous scaling relationships/cost models, the optimum hub height to rotor diameter ratio is predicted. The results of this simulation show that current cost and scaling models do not reflect an accurate optimum height to diameter ratio. However, these cost and scaling models can be modified to provide more accurate predictions of the optimum hub height for a given rotor diameter. This simulation predicts that future large scale wind turbines will have aspect ratios closer to 0.5.

Table of Contents

LIST OF TABLES	vii
LIST OF FIGURES.....	viii
LIST OF SYMBOLS	x
CHAPTER 1: INTRODUCTION	1
1.1 Wind Industry Market Trends.....	1
1.2 Wind Turbine History.....	3
1.3 Wind Turbine Components Overview	3
1.4 Wind Turbine Blades.....	4
1.5 Wind Turbine Foundations	5
1.6 Wind Turbine Towers	6
1.6.1 Lattice towers	6
1.6.2 Concrete towers	7
1.6.3 Tubular towers	7
1.6.4 Hybrid towers	8
1.7 Types of Wind Turbines	9
1.7.1 VAWTs.....	9
1.7.2 HAWTs.....	9
1.8 Previous Research.....	10
CHAPTER 2: THEORY	13
2.1 Wind Model	13
2.2 Weibull Distribution	15
2.3 Maximum Efficiency of the Wind.....	18

2.4	Wind Turbine Power Curves	19
2.5	Annual Energy Production	22
2.6	Levelized Cost of Energy	22
CHAPTER 3: SIMULATION AND MODELING		24
3.1	Simulation Scenario Cases	24
3.1.1	Scenario A – Base Case	25
3.1.2	Scenario B – Modified Cost Model.....	27
3.1.3	Scenario C – Different Location	31
3.2	Average Power Rating	34
3.3	Power Curve Database	35
3.4	Wind Model	40
3.5	Annual Energy Production	41
3.6	Load Factor	42
3.7	Optimization Methods	42
CHAPTER 4: DATA, ANALYSIS, AND RESULTS		45
4.1	Scenario A – Base Case	46
4.2	Scenario B – Modified Cost Model.....	47
4.3	Scenario C – Different Location	49
4.4	Turbine Tower Height Limitations	50
CHAPTER 5: CONCLUSIONS		51
CHAPTER 6: RECOMMENDATIONS FOR FUTURE WORK.....		52
CHAPTER 7: REFLECTIONS.....		53
CHAPTER 8: REFERENCES		54

CHAPTER 9: APPENDIX 59

 APPENDIX A – Cut in, Cut out, and Rated Speed relationships 59

APPENDIX B - Power Curve Trendline Data 60

 APPENDIX C - INITIAL CAPITAL COST BREAKDOWN 61

 APPENDIX D – COE/LF SIMULATION FLOWCHART 63

LIST OF TABLES

Table 1-1. Optimized height vs diameter data set	12
Table 2-1. Common power law exponent values (Ray, Rogers, & McGowan, 2006)	14
Table 3-1. Summary of scenario variables and equations.....	25
Table 3-2. Tower mass scaling equation comparison	28
Table 3-3. Comparison of scenario A and scenario B scaling equation.	29
Table 3-4. Scenario B transportation cost data (National Renewable Energy Laboratory, 2000)	29
Table 3-5. Scenario B transportation subcomponent trendline.....	30
Table 3-6. Subtotal roads and civil cost breakdown for Scenario B	30
Table 3-7. Power curve trendline sample dataset	38
Table 4-1. Summary sheet.....	45
Table 4-2. Percent error between optimization methods and USGS dataset.....	46

LIST OF FIGURES

Figure 1-1. Wind turbine diagram (GE Renewable Energy)	1
Figure 1-2. Newly installed and cumulative wind energy capacity (Global Wind Energy Council, 2017)	2
Figure 1-3. Estimated global electricity production, end-2016 (REN21, 2017).....	3
Figure 1-4. Wind turbine components (Tchakoua P., 2013)	4
Figure 1-5. Patrick and Henderson foundation (Tensionless Pier Wind Turbine Foundation)	5
Figure 1-6. Square pad and pier foundation [1] (National Renewable Energy Laboratory, 2001) [2] (Schaefer, 2011)	5
Figure 1-7. Lattice tower (Big Stone Renewables Services)	6
Figure 1-8. Concrete tower (Florez, 2015).....	7
Figure 1-9. Tubular tower (Tackle TW 1.5S).....	8
Figure 1-10. Hybrid tower (Ozturk, 2016)	8
Figure 1-11. HAWTs vs VAWTs (Ahmed, 2016).....	9
Figure 1-12. USGS onshore turbine hub height vs rotor diameter	10
Figure 1-13. USGS H/D ratio vs rotor diameter	10
Figure 1-14. Optimized height vs diameter	12
Figure 2-1. Wind shear profile.....	13
Figure 2-2. Effect of shape parameter on wind speed distribution	16
Figure 2-3. Effect of scale factor on wind speed distribution	16
Figure 2-4. Weibull shape parameter vs annual average wind speed (Homer Energy)	17
Figure 2-5. Nominal turbulence vs. wind speed (Larson & Hansen, 2001)	17
Figure 2-6. Wind control volume around a turbine (Schmidt, 2007)	18
Figure 2-7. Coefficient of performance as a function of v_2/v_1 (Schmidt, 2007).....	19
Figure 2-8. Typical power curves	19
Figure 2-9. Power output and coefficient of performance	21
Figure 2-10. Turbulence intensity effect on wind turbine power curve (Clifton & Wagner, 2014)	21
Figure 3-1. <i>WindPACT Design Cost and Scaling Model</i> cost breakdown sample	26

Figure 3-2. Simulated cost breakdown sample.....	27
Figure 3-3. Seven Mile Wind Farm site location for Scenario C (PacifiCorp, 2011).....	31
Figure 3-4. Oklahoma City, Oklahoma wind rose profile (National Water & Climate Center, 2002)	32
Figure 3-5. Rock Springs, Wyoming wind rose profile (National Water & Climate Center, 2002).....	33
Figure 3-6. USGS Dataset Power Rating vs Diameter	34
Figure 3-7. USGS Dataset Power Rating vs Height	35
Figure 3-8. Power curves for all turbines at 1000kW	36
Figure 3-9. Power curve relationship for increasing rotor diameter at constant power rating	36
Figure 3-10. Power curves for all turbines with 70 m rotor diameter	37
Figure 3-11. Power curve range for 70 m rotor diameter.....	37
Figure 3-12. Model Validation using Suzlon S60/1000 power curve	39
Figure 3-13. Weibull distribution calculation spreadsheet	40
Figure 3-14. Annual energy production trends.....	41
Figure 3-15. AEP local maxima.....	41
Figure 3-16. Load factor trends.....	42
Figure 3-17. COE optimization method sample graph.....	43
Figure 3-18. COE optimization method at constant height	43
Figure 3-19. COE/LF optimization method sample graph	44
Figure 4-1. Optimum diameter given height method	45
Figure 4-2. Scenario A optimum height vs diameter.....	46
Figure 4-3. Scenario A – Cost breakdown	47
Figure 4-4. Scenario B – Cost breakdown	47
Figure 4-5. Scenario B height vs diameter.....	49
Figure 4-6. Scenario B height vs diameter of all optimization methods.....	49
Figure 4-7. Scenario B and Scenario C height vs optimum diameter comparison	50

LIST OF SYMBOLS

A	Area	(m ²)
AEP	Annual Energy Production	(kWh)
c	Scale Factor	
COE	Levelized Cost of Energy	(\$/kWh)
Cp	Coefficient of Performance	
d	Diameter	(m)
FCR	Fixed Charge Rate	
h	Height	(m)
ICC	Initial Capital Cost	(\$)
k	Shape Parameter	
LF	Load Factor	
LLC	Land Lease Cost	(\$/kWh)
LRC	Levelized replacement Cost	(\$)
m	Meters	
ṁ		
OH	Operating Hours	(h)
OM	Operation and Maintenance Cost	(\$/kW)
P	Power	(kW)
PR	Power Rating	(kW)
s	Seconds	
U(z)	Target Height Wind Speed	(m/s)
U(z _r)	Reference Height Wind Speed	(m/s)
v	Wind Speed	(m/s)
v̄	Annual Average Wind Speed	(m/s)
Ẃ	Kinetic Energy	(kJ)

Z	Target Height (m)
Z_r	Reference Height (m)

Greek Symbols

α	Power Law Exponent
Γ	Gamma Function
ρ	Density (kg/m ³)

CHAPTER 1: INTRODUCTION

The wind industry is a fast growing market and could one day provide more energy than the nuclear or coal industry (US Energy Information Administration, 2018). In order for wind energy to compete with other non-renewable resources it must become be very cheap and very efficient. A lot of previous research has been done to help identify certain design parameters and to optimize each turbine component. Optimization is very important in the energy industry because it is all about reducing capital cost to stay competitive. One particular area of optimum wind turbine design is the tower hub height to rotor diameter aspect ratio. Current design standards set a fixed rate of 1-1.3 for the height to diameter ratio as this is the estimated best ratio to receive the most power output for the least cost.

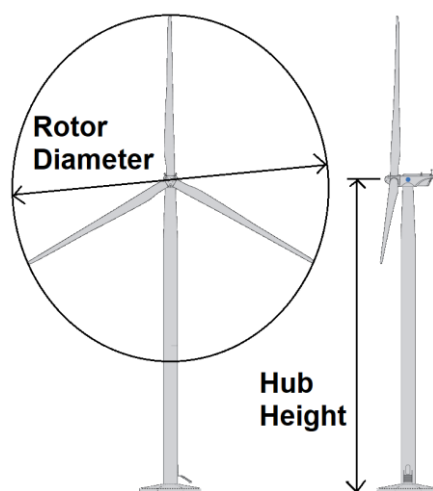


Figure 1-1. Wind turbine diagram (GE Renewable Energy)

1.1 Wind Industry Market Trends

The wind industry is the second fastest growing renewable energy source next to solar energy which only passed the wind industry at the beginning of 2017. By 2022 growth in renewable generation will be twice as large as that of gas and coal combined (International Energy Agency, 2017). The growth in renewable energy is spurred by the changes in global policy for a cleaner energy sources and a reduced dependence on quickly diminishing coal and gas reserves. With the advancements in wind turbine technology, the price for wind energy is quickly becoming competitive with traditional non-renewable sources (Shahan, 2016).

These growing global trends are spurred by China, the United States, and Germany who together hold 62% of the cumulative wind energy capacity. The United States wind industry alone installed 7,017 MW of new wind capacity bringing the total to 89,077 MW of cumulative installed wind capacity by the end of 2017. There are more than 54,000 wind turbines operating in 41 states plus Guam and Puerto Rico (American Wind Energy Association, 2017). The US holds 17% of the global cumulative installed capacity which is only second to China at 35% of the global installed wind capacity by the end of 2017 (Global Wind Energy Council, 2017).

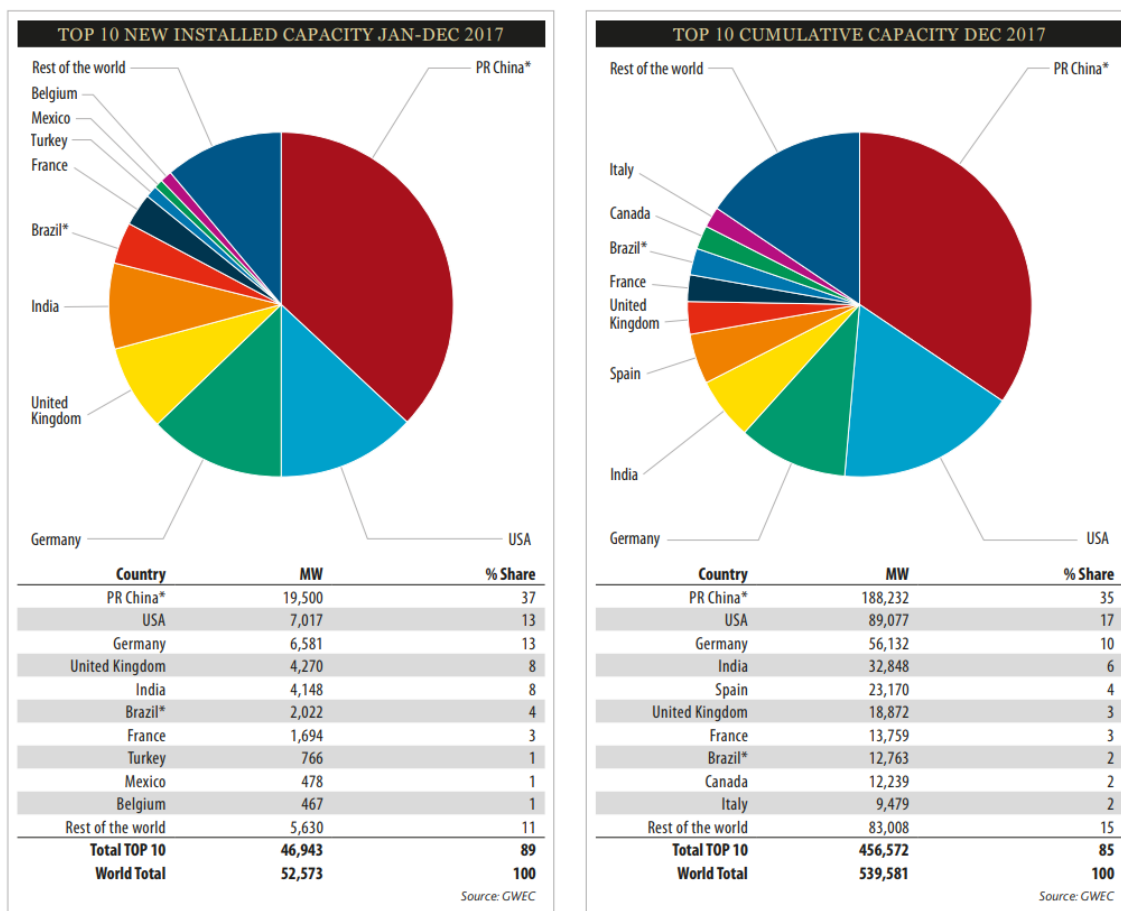


Figure 1-2. Newly installed and cumulative wind energy capacity (Global Wind Energy Council, 2017)

Despite the positive outlook on the growth potential of wind power, only 4% of the global electricity production came from wind power by the end of 2016 and 75.5% of the electricity production were from non-renewable sources (REN21, 2017). Additionally, the wind industry has only been prevalent since the 1970s (Wind Energy Foundation) whereas the nuclear industry began in the 1940s (World

Nuclear Association, 2018) and the coal industry can date back as far as the mid-19th century. The wind industry is much younger than other traditional non-renewable resources and has only recently become highly competitive.

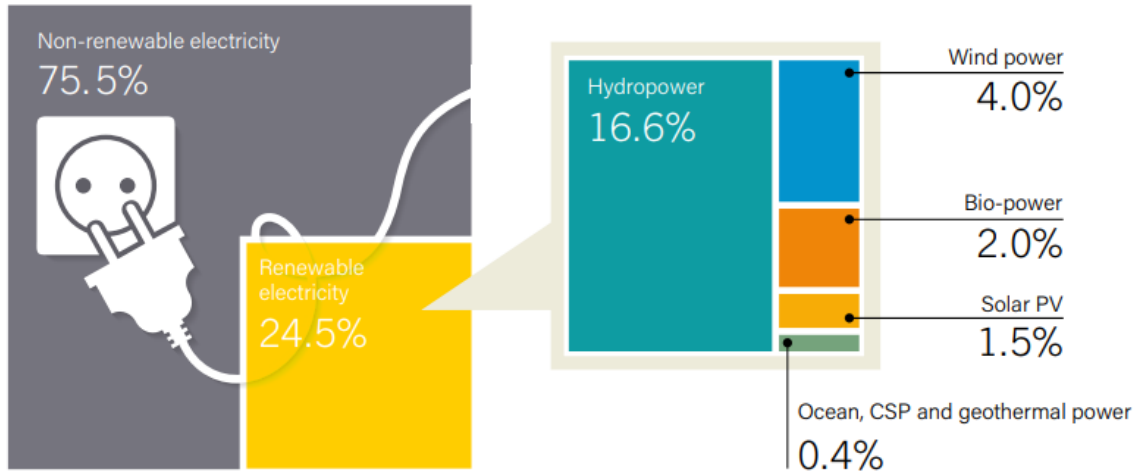


Figure 1-3. Estimated global electricity production, end-2016 (REN21, 2017)

1.2 Wind Turbine History

Although the technology used to generate power using the wind is very young, the principles of harnessing wind power have been utilized since early recorded history. Wind has been used to propel boats, pump water, and grind grain through simple windmills that were developed in early China. Windmills were never a primary source of electrical energy until the mid-1970s when there was a revival of the wind industry as people began looking for alternate sources of energy (Wind Energy Foundation). The main difference between the windmills of the past and modern wind turbines are the shape and material design of the blades. Historical windmills have many large, flat blades which operated similarly to boat sails. Today's turbines feature three aerodynamically shaped blades used to efficiently capture the wind.

1.3 Wind Turbine Components Overview

Modern turbines include several main components: the tower, foundation, blades, gearbox, generator, and transformer. As the wind blows across the rotor blades, a pressure gradient is formed between the upwind and downwind sides of the blade causing a resulting lifting force which pushes the blades clockwise around the main shaft. Through a series of gears, the slow main shaft (30-60 rpm) is

translated into the high speed output shaft (1,000-1,800 rpm) which is connected to the generator. The generator is a typical induction generator which produces AC electricity. The electricity produced from the generator is amplified by a step-up transformer in the power electronics system to reach the required output voltage needed to supply the power grid (US Department of Energy).

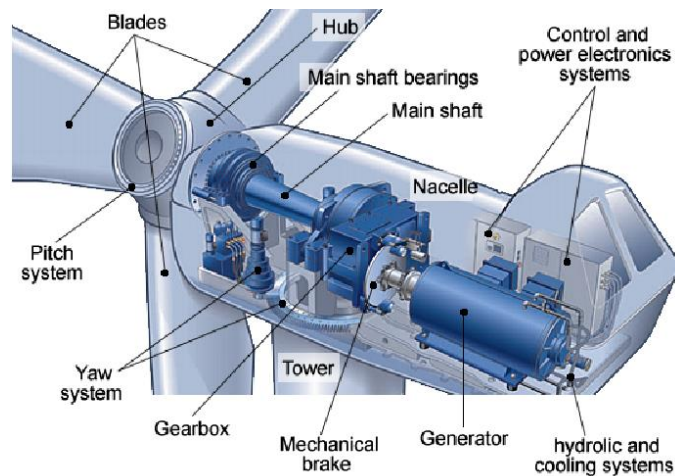


Figure 1-4. Wind turbine components (Tchakoua P., 2013)

This thesis focuses on the length of the turbine blades and the tower height; as such each of these components will be described in further detail below.

1.4 Wind Turbine Blades

For the purpose of this thesis, the aerodynamics of the turbine blades are not considered. The only factor that was changed was the length; it was assumed that the airfoil blade properties such as chord length, thickness, and twist angle are appropriately scaled during the experiment. The current wind turbine blade manufacturing process uses an injection moulding technique which allows complex geometries to be assembled with relative ease. With that in mind it was assumed that any size turbine blade could be produced up to a theoretical 100 meters in length (200 m in diameter) based on current and future blade length sizes. The current largest blade length is the MHI Vestas V164-9.5 which has an 80 m blade length and is atop of a 105 m tower (Aarhus, 2017). Future blade lengths will surpass 100 m in length based on GE's proposed Haliade-X which will have a 107 m blade on top of a 260 m tower (Kellner, 2018).

1.5 Wind Turbine Foundations

The two turbine foundations considered in this thesis are the Patrick and Henderson Tensionless Foundations design and a square pad-and-pier foundation. The Patrick and Henderson Foundation is made by placing an inner and outer concentric corrugated metal pipes into the soil. In between the pipes is a metal anchor cage that is later filled with concrete. The foundation is approximately 4.5 m in diameter and 9 m deep. The P&H foundation offers a smaller material footprint and can be adaptable to poorer soil conditions (Miceli, 2012). The square pad and pier foundation is made by pouring concrete into a circular or octagonal shaped foundation pad which is filled with structural steel caging. The diameter and thickness of the pad are dependent on the combined weight of the turbine and tower to prevent overturning. The upper pier of the foundation has supporting bolts embedded into the concrete to connect to the steel tubular tower. The pad and pier foundation uses much more concrete than the P&H foundation but can be installed in shallow ground.

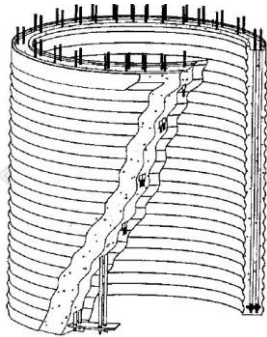
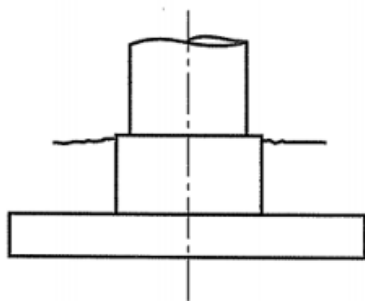


Figure 1-5. Patrick and Henderson foundation (Tensionless Pier Wind Turbine Foundation)



[1]



[2]

Figure 1-6. Square pad and pier foundation [1] (National Renewable Energy Laboratory, 2001) [2] (Schaefer, 2011)

1.6 Wind Turbine Towers

Typical tower designs include lattice towers, concrete towers, tubular towers, and hybrid towers. When determining the optimum tower height for a given rotor diameter within the simulation, no physical static or fatigue analysis was done on the structural integrity of the tower. It should be noted that a common misnomer is that there is a 500 ft. height limit (from the base of the tower to the tip of the blade at its highest point) on all wind turbine towers as regulated by the Federal Aviation Administration (FAA). The FAA only requires that an aeronautical study be performed to determine whether or not the structure will interfere with known aircraft flight paths (Federal Aviation Administration, 2018). With this in mind it was proposed that the tower heights could be constructed up to a theoretical 200 meters.

1.6.1 Lattice towers

Lattice towers are manufactured using welded steel profiles. The truss action and larger base dimensions help resist the applied loads more effectively. Additionally the open tower leads to reduced wind loads on the structure. The small tower pieces are cheap to manufacture and can easily be transported to the site. The downside to lattice towers is the steep on-site construction cost because of the quantity of pieces needed to assemble. Also the maintenance cost for lattice towers is quite high as each joint offers a possibility of failure, especially in colder climates where icing can occur (Attar, 2012).



Figure 1-7. Lattice tower (Big Stone Renewables Services)

1.6.2 Concrete towers

The primary advantages of concrete towers are increased durability, lower maintenance costs, and a versatile design that can be implemented into almost any turbine requirement. Concrete towers can also be segmented in almost any orientation to allow for simplified transportation. However concrete towers require a longer on-site construction time depending on the assembly method used. Also there is a high probability of failure as cracks can easily propagate during the curing process (Jimeno).



Figure 1-8. Concrete tower (Florez, 2015)

1.6.3 Tubular towers

Most utility scale wind turbines are affixed on top of a tubular steel tower. Tubular towers are made up of two to ten steel rolled tower sections ranging anywhere from 1.5-5 m in diameter. The tower sections are generally around 20-30 meters in length and have flanged ends that allow for simple bolted connection which greatly reduces on-site assembly. Tubular towers are conical in shape with the base of the tower decreasing in size towards the top of the tower. This thesis uses a tubular tower for all tower design considerations up to heights of 200 meters.

For larger tubular towers there are some design considerations that were dismissed for the scope of this project. There currently exist limitations for road transportation because of bridges and other obstacles that restrict the tower base diameter to approximately 4.5 meters. It was found that for towers above 85 m in height exceeded the transportation base diameter restriction. To transport tubular tower sections larger than 85 m in height the larger sections can

be halved or quartered lengthwise. This would allow the tower sections to be transported while remaining within the 4.5 meter height limit. These costs for the additional on-site assembly of larger towers are built into the cost analysis scenario (Nicholson, 2011).



Figure 1-9. Tubular tower (Tackle TW 1.5S)

1.6.4 Hybrid towers

Hybrid towers are generally a combination of concrete and tubular or lattice and tubular towers. At very tall tower heights the base diameter for a standard tubular tower would exceed transportation limits. By supplementing the bottom section of the tower with the stronger concrete or lattice base this could reduce overall remaining tower cost and increase the annual power output of the turbine.



Figure 1-10. Hybrid tower (Ozturk, 2016)

1.7 Types of Wind Turbines

Modern turbines are divided into two categories: Horizontal Axis Wind Turbines (HAWTs) and Vertical Axis Wind Turbines (VAWTs) (Figure 1-11). Most utility scale wind farms use horizontal axis turbines, therefore for the purpose of this thesis only HAWTs will be considered.

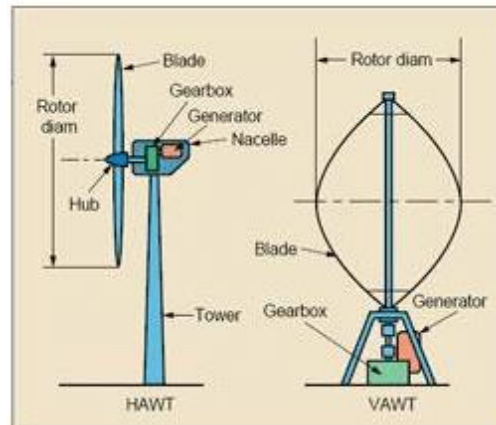


Figure 1-11. HAWTs vs VAWTs (Ahmed, 2016)

1.7.1 VAWTs

Vertical axis wind turbines are oriented so that the main rotor shaft is transverse to the wind and the majority of the components are at the base of the turbine. The blades are oriented vertically which allows them to catch the wind from any direction. However, when wind is blowing on one side of the turbine the blades on the far side of the turbine do not contribute to the output power that is generated thereby reducing efficiency. An advantage for VAWTs is that they do not need the complex wind detecting sensors that are common on HAWTs to help orient them in the direction of the wind. Lastly, VAWTs are designed to operate in gusty conditions at high wind speeds.

1.7.2 HAWTs

HAWTs in contrast to VAWTs have the main rotor shaft on the top of the tower oriented perpendicular to the ground. The main advantages to HAWTs are its fully automated control systems, efficient power usage, and long life cycle of up to 20 years in the field. Each of the wind turbines are equipped with wind sensing technologies that help position the blades in the direction of the wind. Not only does the upper motor housing or nacelle rotate to position the blades into the wind (yaw), but each blade can rotate (pitch) to improve power output and efficiency. By

orienting the tower into the wind, the control systems are able to reduce unnecessary fatigue stresses on the blades from crosswind and help extend the life cycle of the wind turbine.

1.8 Previous Research

The United States Geological Survey department provides open source data for various energy sources within the US. The USGS has compiled a detailed database (United States Geological Survey, 2016) of almost every turbine that was installed in the United States up to 2014. Using this database the relationship of hub height to rotor diameter was investigated and is summarized in Figure 1-12. Using the same dataset the ratio of H/D is presented in Figure 1-13. While the USGS dataset does not include all turbines, it can be concluded that the current hub height to rotor diameter ratio of a turbine varies between .5 and 1.7.

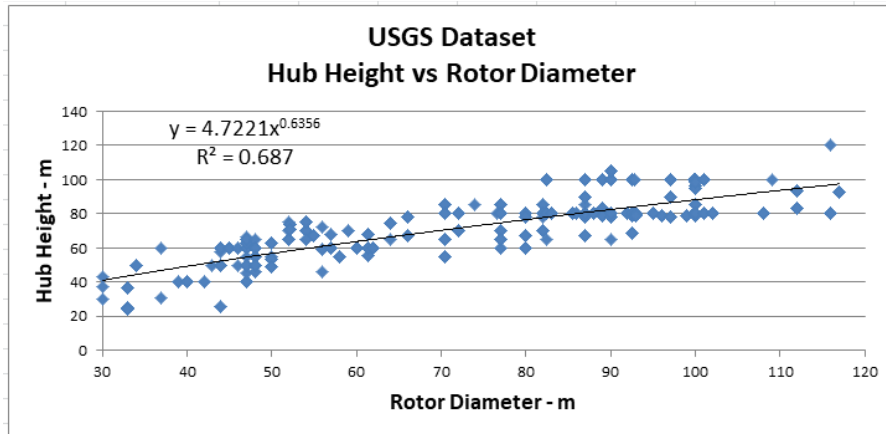


Figure 1-12. USGS onshore turbine hub height vs rotor diameter

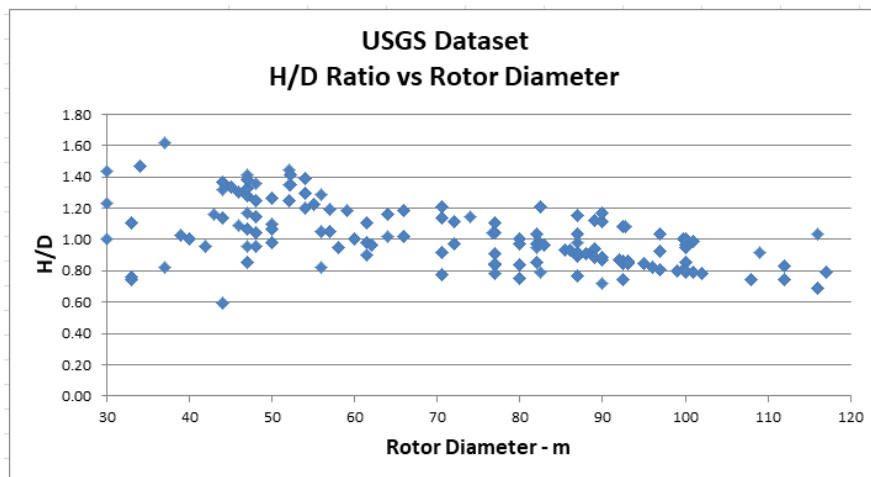


Figure 1-13. USGS H/D ratio vs rotor diameter

While a lot of research has been done on refining the many wind turbine parameters, there is no definite rule or solution which determines the optimum hub height for any given diameter. A report from a Swedish research program *Vindforsk* says that “a general rule of thumb has been to furnish a wind turbine with a tower as tall as the turbine diameter, with deviations downwards for high wind speed sites.” They later refine their statement to say that “it is economical to build taller towers than the hitherto conventional one turbine diameter.” This particular study attempted to optimize the hub height for a 3 and 5 MW turbine. They analyzed multiple different types of towers and found that one of the main limiting factors on tower hub height were crane height limitations. Current crane technologies are only economical up to 120-150 m hub heights where above this height requires specialized lifting towers. The other main limiting factor was that the maximum allowable diameter for the tower sections was 4.5 meters in order to easily transport them across roadways and under bridges. Above this diameter, the tower sections had to be quartered and re-assembled on site (Engström, 2010).

The *WindPACT Technical Area 2* report was conducted by the National Renewable Energy Laboratory whose purpose was to help “determine the optimum sizes for future turbines [and] help define sizing limits for certain critical technologies.” In this report “the hub height was fixed across each turbine by the hub height to rotor diameter ratio of 1.3. Current design practices use ratios between 1 and 1.3.” The rest of the report details other turbine scaling relationships and how they were derived, yet the above statements are all that is listed for the hub height to rotor diameter ratio (National Renewable Energy Laboratory, 2000).

The *Distributed Wind Energy Association* states that “the lowest extension of a wind turbine rotor must be 60 feet above the ground, assuming no surrounding obstacles. Where obstacles are present, the wind turbine rotor should be at least 30 feet above the tallest obstacle within a 500-foot radius.” No specific guidelines are given as to the optimum height based on turbine size or rotor diameter, these minimum turbine height guidelines were “based on decades of experience that includes tens of thousands of wind turbine installations” (Distributed Wind Energy Association, 2014).

Figure 1-14 and Table 1-1 summarize the optimum rotor diameter to hub height ratio of two notable optimization reports. It should be noted that this information is not based on extensive datasets; rather these particular thesis's attempted to find the optimum design parameters for 4-5 turbines.

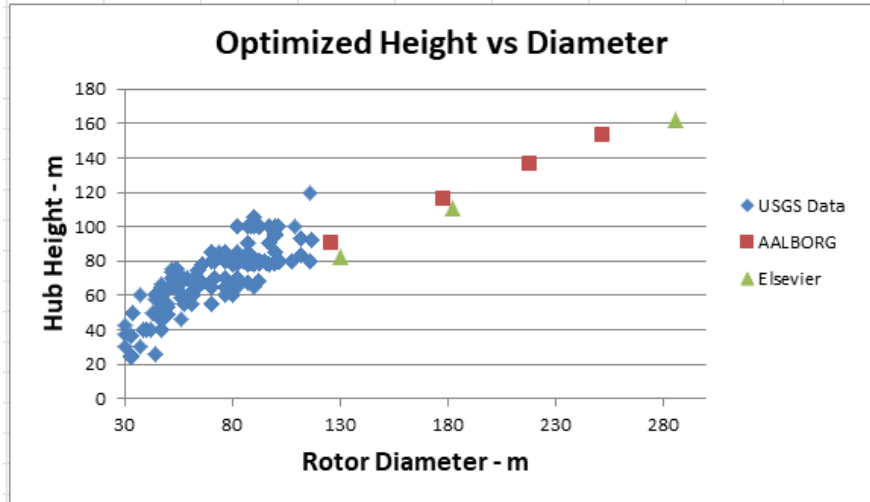


Figure 1-14. Optimized height vs diameter

Elsevier (Ashuri, 2016)		AALBORG (Bulder, 2012)	
D	H	D	H
130	82.4	126	90
182	110.4	178	116
286	162	218	136
		252	153

Table 1-1. Optimized height vs diameter data set

With this information in mind, this thesis will attempt to expand upon this gap in literature surrounding the optimal hub height to rotor diameter ratio.

CHAPTER 2: THEORY

This section will detail the background principles for calculating wind turbine energy production and cost of energy that was used in this thesis. It will describe how the primary equations were derived and how they are implemented into the simulation.

2.1 Wind Model

For the purpose of this thesis, an approximation of the wind speed at any given height was required. The most accurate wind estimation methods would be to use remote sensing such as collecting SODAR or LIDAR data at the geographical location and height of the newly proposed turbine. However oftentimes this is not feasible and predictions of the new location must be based on extrapolated data from the measured location.

The flow of wind over the earth's surface can be modeled by a viscous fluid boundary layer over a flat plate. The velocity profile of the wind as it approaches a wind turbine would look similar to Figure 2-1.

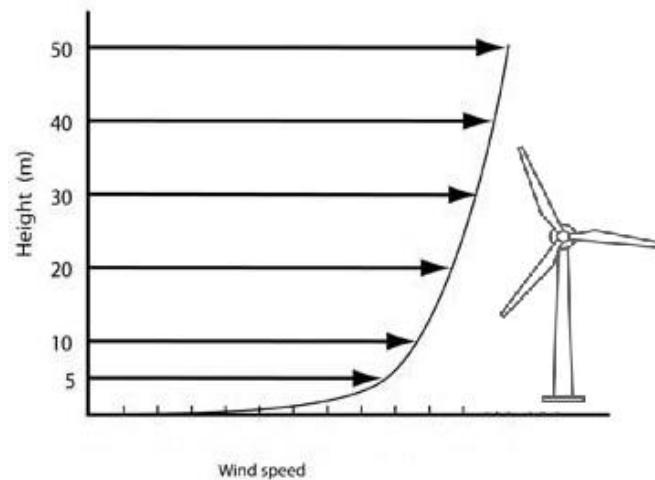


Figure 2-1. Wind shear profile

Wind shear profiles are dependent on the speed of the wind, the height above the ground, the ground's surface roughness, the ground's roughness variation, the atmospheric stability, and the geographical elevation. Current models exist to estimate the wind profile at any given height; the two common wind shear models are the log law and the power law. Previous literature has shown that there is no significant difference in performance between the log and power laws. Either wind shear model will

be within 5% of the true hub height mean wind speed (Ray, Rogers, & McGowan, 2006). The model used in this thesis is the more commonly used power law.

$$\frac{U(Z)}{U(Z_r)} = \left(\frac{Z}{Z_r}\right)^\alpha \quad (1)$$

where

$U(z)$ = target height wind speed (m/s)

$U(z_r)$ = reference height wind speed (m/s)

Z = target height (m)

Z_r = reference height (m)

α = power law exponent

Current meteorological data exists for wind speeds at a standard 10 m height at various locations across the United States (Standardized Extreme Wind Speed Database for the United States, 2016). This data can be used to determine the reference height and wind speed in a similar region that the proposed wind turbine will be sited. The power law exponent is dependent on the surface roughness of the region and must be estimated based on previous literature on surface roughness. Typical values for the power law exponent based on varying terrains are given by Table 2-1

Terrain Description	Power law exponent, α
Smooth, hard ground, lake or ocean	0.10
Short grass on untilled ground	0.14
Level country with foot-high grass, occasional tree	0.16
Tall row crops, hedges, a few trees	0.20
Many trees and occasional buildings	0.22 – 0.24
Wooded country – small towns and suburbs	0.28 – 0.30
Urban areas with tall buildings	0.4

Table 2-1. Common power law exponent values (Ray, Rogers, & McGowan, 2006)

It should be noted that the wind shear coefficient varies throughout the day, by season, and even with the weather. Studies have shown that by using a variable wind shear coefficient over a fixed wind shear coefficient improvements range from 4% to 41% between predicted and actual wind speeds at higher hub heights (Corcadden, 2016). For simplification, this thesis uses a constant power law exponent when calculating the wind speed at varying heights.

2.2 Weibull Distribution

At any wind turbine site the wind speed and direction varies throughout the day. Varying wind directions would require the wind turbine to yaw into the wind as needed. To simplify the simulation, it was assumed that the wind turbine was always facing the headwind and incurred no losses due to lagging dynamic yawing control. To account for varying wind speeds, long term wind speed data must be collected on site. It has been found that Weibull and Rayleigh functions appear to accurately reflect the wind speed probability datasets (Nielsen, 2011). Weibull and Rayleigh distributions measure how much time of the year (in percent) that each wind speed occurs. The Weibull distribution is the most widely used probability density function and is defined as:

$$Weib(v) = \frac{k}{c} \left(\frac{v}{c}\right)^{k-1} e^{-\left(\frac{v}{c}\right)^k} \quad (2)$$

where

k = shape parameter

v = wind speed (m/s)

c is the scale factor and is given by:

$$c = \frac{\bar{v}}{\Gamma\left(1+\frac{1}{k}\right)} \quad (3)$$

where

\bar{v} = annual average wind speed (m/s)

Γ represents the Gamma function

When the shape parameter is equal to 2, the Rayleigh distribution is obtained; this distribution is used in the studies in the international standard IEC 61400-12-1 (Carillo, 2014). Figure 2-2 shows the effect of varying the shape parameter on a typical Weibull distribution plot. Similarly, Figure 2-3 shows the effect of varying the scale factor in a Weibull plot.

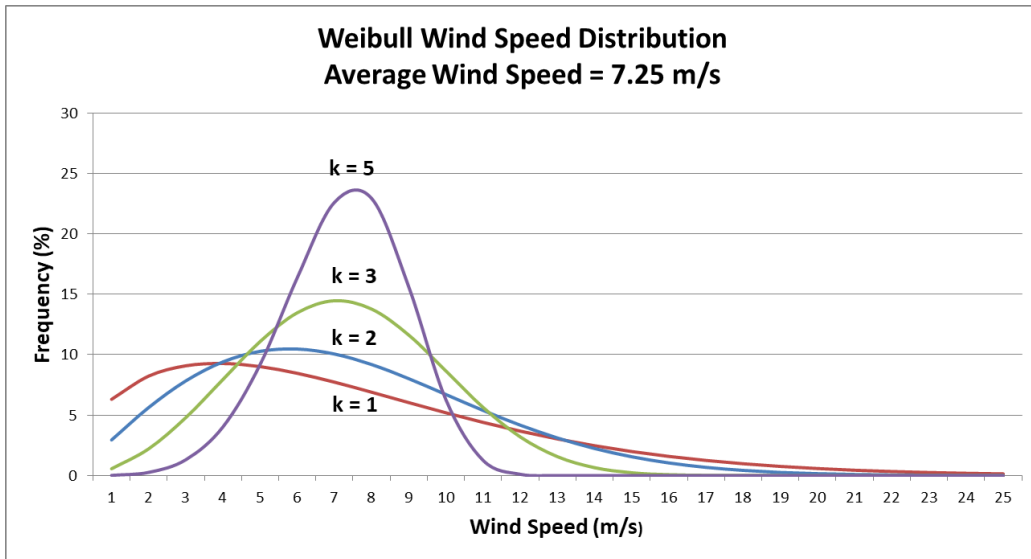


Figure 2-2. Effect of shape parameter on wind speed distribution

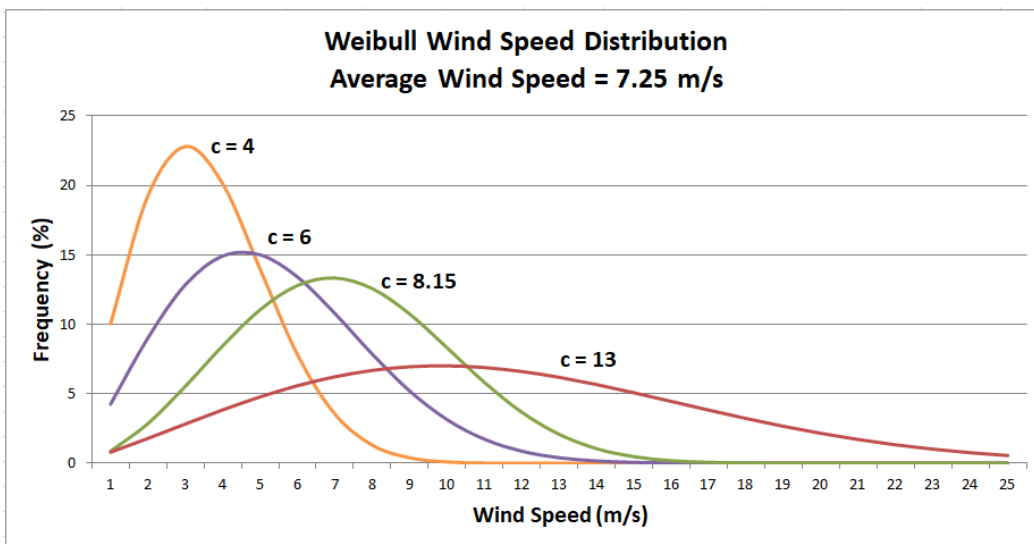


Figure 2-3. Effect of scale factor on wind speed distribution

The shape factor k is a parameter used to relate how consistent the wind speeds are in the Weibull distribution plot. For example a very gusty, mountainous region might have a Weibull k value as low as 1.5. However, the steady, tropical wind just off the coast can have a Weibull k value up to 3 or 4 (Homer Energy). Figure 2-4 shows a correlation between increasing wind speeds and the shape parameter. It was also proven in Figure 2-1 that the wind speeds increase with increasing height. Therefore it can be concluded that the shape factor k scales with height.

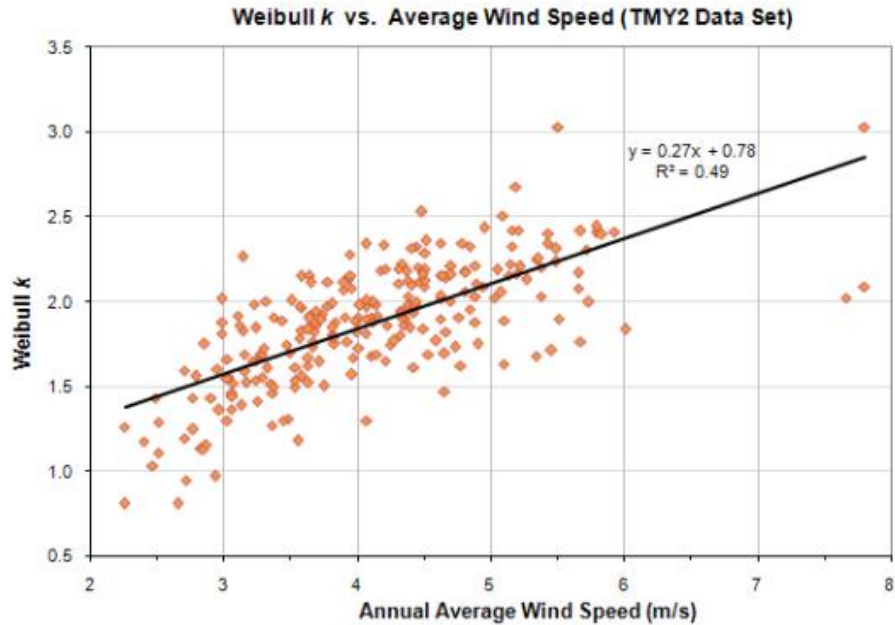


Figure 2-4. Weibull shape parameter vs annual average wind speed (Homer Energy)

This correlation can be validated by Figure 2-5 since the turbulence intensity is shown to decrease at higher wind speeds. Higher wind speeds means less turbulence and more consistent winds (higher k value). Turbulence intensity is defined as the standard deviation of the horizontal wind speed divided by the average wind speed over some time period, typically 10 minutes (Lundquist & Clifton, 2012).

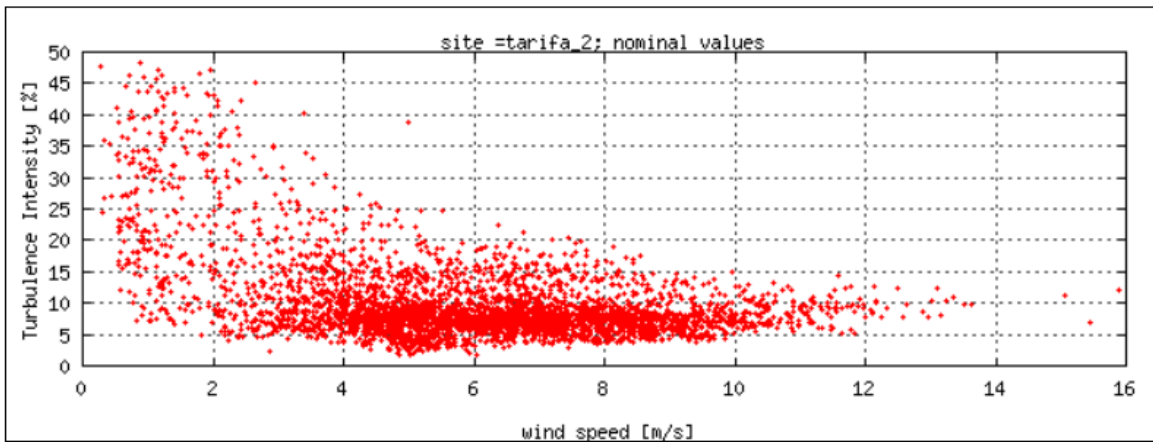


Figure 2-5. Nominal turbulence vs. wind speed (Larson & Hansen, 2001)

2.3 Maximum Efficiency of the Wind

A wind turbine converts the kinetic energy of the wind into mechanical energy through the spinning blades. However there is a theoretical maximum amount of energy that can be extracted from the wind. Figure 2-6 shows a profile view of a wind turbine and the control volume around a wind turbine.

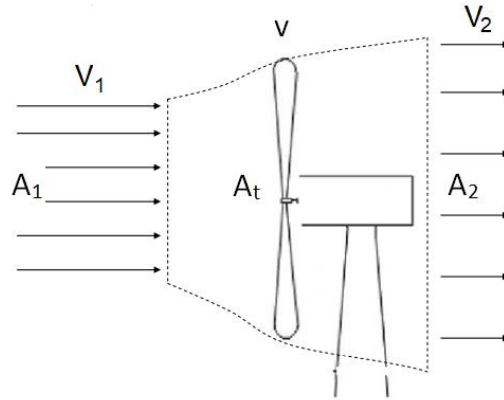


Figure 2-6. Wind control volume around a turbine (Schmidt, 2007)

Since the air is incompressible, the mass flow rate of air \dot{m} can be defined as:

$$\dot{m} = \rho A_1 v_1 = \rho A_t v = \rho A_2 v_2 \quad (4)$$

where ρ is the density of air.

The rate at which kinetic energy is extracted from the wind by the turbine is equal to the loss in kinetic energy of the wind before and after the turbine.

$$\dot{W} = \frac{1}{2} \dot{m} (v_1^2 - v_2^2) \quad (5)$$

Combining the mass flow rate at the turbine from Eq. 4 into Eq. 5 and knowing from the actuator disc theory that v at the turbine is equal to the average of the wind velocity before and after the turbine gives Eq. 6 (Blackwood, 2016).

$$\dot{W} = \frac{1}{2} \left[\rho A_t \left(\frac{v_1 + v_2}{2} \right) \right] (v_1^2 - v_2^2)$$

Which simplifies into:

$$\dot{W} = \frac{1}{2} \rho A_t v_1^3 C_p \quad (6)$$

where C_p is the coefficient of performance and is given by:

$$C_p = \frac{\left(1 + \frac{v_2}{v_1}\right) \left[1 - \left(\frac{v_2}{v_1}\right)^2\right]}{2} \quad (7)$$

Figure 2-7 shows the coefficient of performance plotted against v_2/v_1 and the theoretical max C_p occurs when v_2/v_1 is equal to $1/3$ and the C_p is equal to $16/27$ or approximately 59%. This is referred to as Betz's Law and proves that the maximum power that can be extracted from the wind, independent of the design of a wind turbine in open flow is 59%.

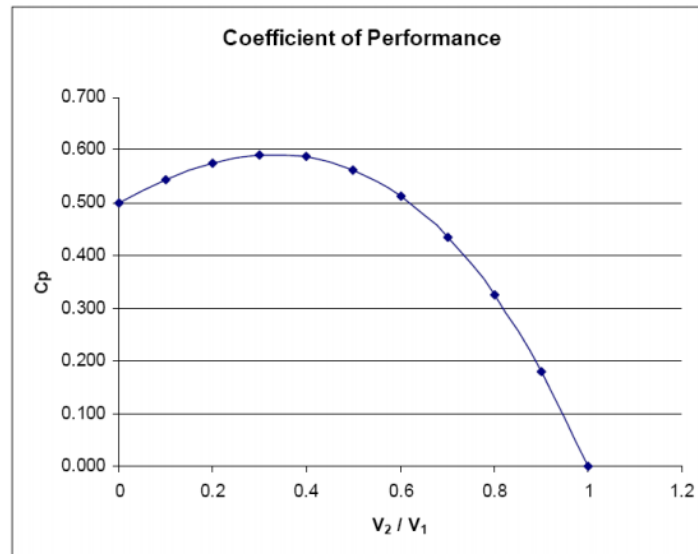


Figure 2-7. Coefficient of performance as a function of v_2/v_1 (Schmidt, 2007)

2.4 Wind Turbine Power Curves

The output power generated from a wind turbine can be characterized by a unique power curve which compares the output power (kW) to the average wind speed (m/s). A typical power curve is shown in Figure 2-8. This particular turbine has a 2 MW power rating with 70 m rotor diameter.

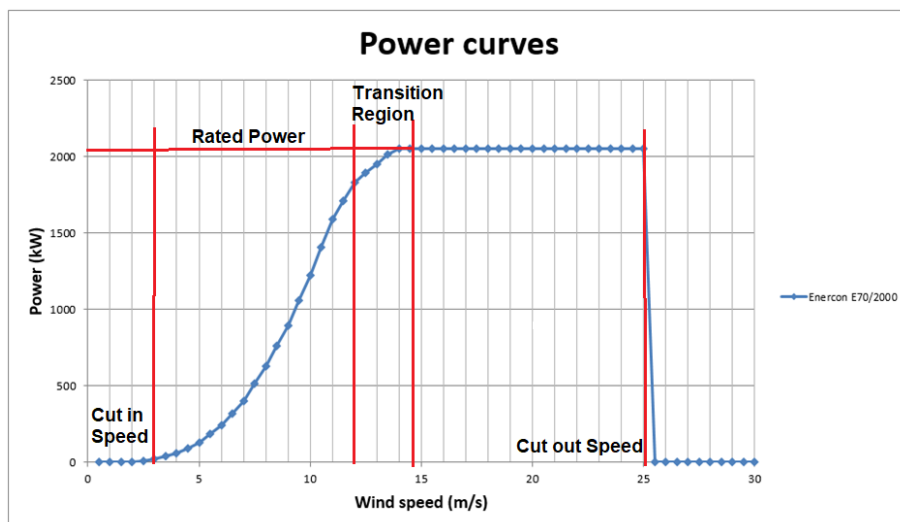


Figure 2-8. Typical power curves

A power curve can be divided into four main sections based on the cut-in speed, the rated power, and the cut-out speed. The power output at each of these sections is summarized by the piecewise function below:

$$P(v) = \begin{cases} 0 & , v < \text{cut in speed} \\ \frac{1}{2} \rho A_t v_1^3 C_p & , \text{cut in speed} \leq v \wedge P(v) < \text{rated power} \\ \text{rated power} & , P(v) \geq \text{rated power} \\ 0 & , v \geq \text{cut out speed} \end{cases} \quad (8)$$

The cut in speed is the minimum wind speed at which a turbine will generate power, generally between 3 and 5 m/s. The rated power is the maximum power which the turbine can produce; most turbines are identified by their power rating. The cut out speed (≈ 25 m/s) is the fastest wind speed that the wind turbine will produce power, any higher wind speeds and the turbine will pitch the blades out of the wind to help to stall the turbine. This stalling technique is used to reduce fatigue damage on the blades during high winds (Wan, Ela, & Orwig, 2010). It should be noted that the transition region specified by Figure 2-8 is not operating at peak power output as the blades are adjusted to reduce the power output to match the rated power.

Generally a power curve will be provided by the manufacturer of a particular wind turbine and the coefficient of performance must be extrapolated from the data. Since data about the wind speeds before and after a turbine are not widely available to estimate the turbine efficiency the ratio of power provided by the turbine to the maximum available power from the wind (Eq. 9) is used. This ratio is plotted for the Suzlon S64/1000 turbine (Figure 2-9) which has a rotor diameter of 64 m and a rated power of 1000 kW. Note how the maximum efficiency for this particular turbine is approximately .45 which is below the Betz's theoretical maximum efficiency for a turbine at 59%. Most turbines range between 35-45% efficiency.

$$C_p = \frac{\text{Power generated by wind turbine}}{\text{Theoretical max power available in wind}} \quad (9)$$

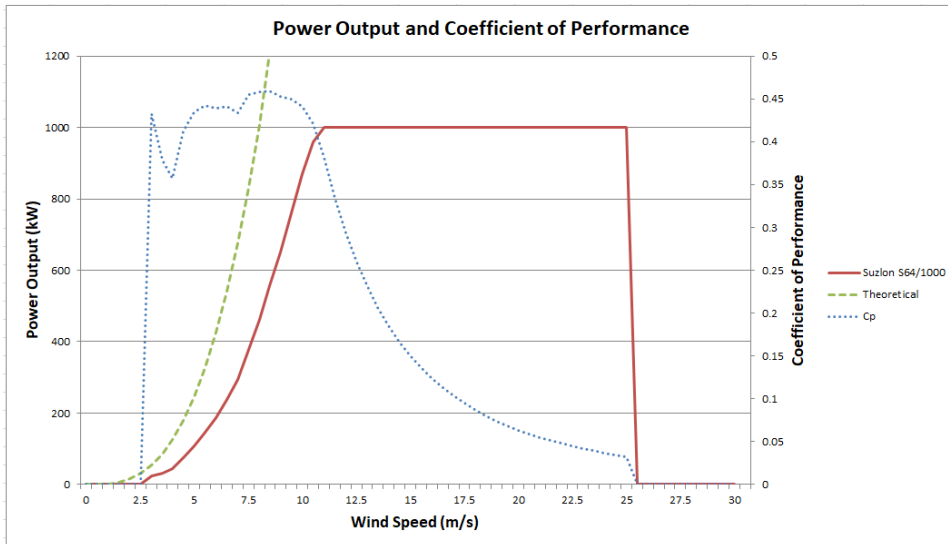


Figure 2-9. Power output and coefficient of performance

Recent research has shown that the power output of wind turbines can vary dramatically at the same 10-minute average wind speed, as turbulence and other inflow characteristics change (Clifton & Wagner, 2014). Turbulence always decreases the total output power and the effect of varying turbulence intensities on the power curve is described in Figure 2-10. The International Electrotechnical Commission 61400-12-1 report states that the “standard for power curve evaluation recognizes only the mean wind speed at hub height and the air density as relevant to the power production” (Hedevang, 2014). While acknowledging the negative impact of the turbulence intensity on the power output of a turbine, this thesis will follow the IEC 61400 standard and not factor it into the final power output calculations.

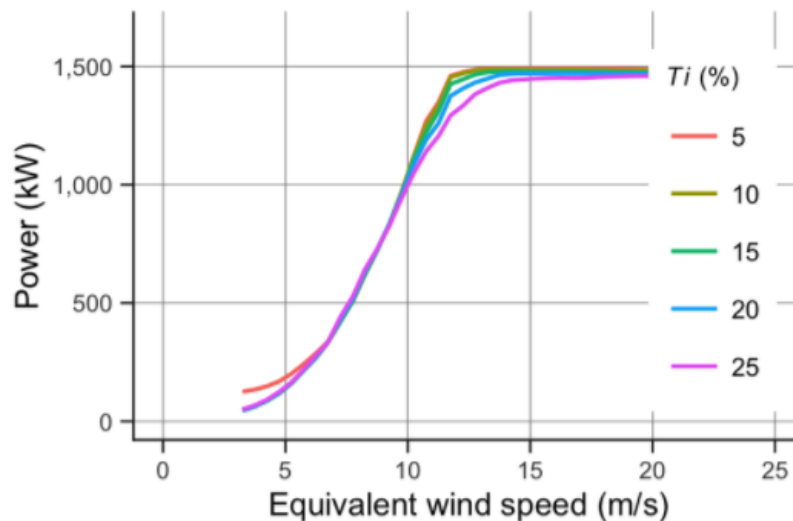


Figure 2-10. Turbulence intensity effect on wind turbine power curve (Clifton & Wagner, 2014)

2.5 Annual Energy Production

Annual Energy Production or AEP is the total amount of energy (kWh) that a turbine produces in one year. To calculate AEP, a specific turbine's power curve and the Weibull wind speed distribution of the turbine site will be needed. The Weibull wind speed distribution provides the percentage of the year (assuming the wind data is averaged over a one year period) that the wind speeds are blowing at the specified rates. Since this simulation calculates the AEP for all wind speeds between 0 and 30 m/s there is a percentage of the year that the wind is below the cut in speed and above the cut out speed for a particular turbine. To account for this, the operating hours (OH) of the turbine are calculated as number of hours per year that the wind is blowing between the cut in speed and cut out speed based on the Weibull distribution of the wind profile. Equation 10 combines Equation 2 and Equation 8 to yield the Annual Energy Production:

$$AEP = \sum_{v=\text{cut in speed}}^{\text{cut out speed}} P(v) * Weib(v) * OH \quad (10)$$

A common way to compare the energy output between turbines is to use a load factor or capacity factor. The load factor (LF) is a non-dimensional unit that compares the actual energy produced by the turbine to the total possible energy produced by the turbine if it were operating all year (8760 hours) at its power rating (PR). A high load factor correlates to a more efficient turbine.

$$LF = \frac{AEP}{PR * 8760} \quad (11)$$

2.6 Levelized Cost of Energy

The levelized cost of energy (LCOE or COE) measures the lifetime costs of an energy source divided by the output energy production. This allows a simple, accurate comparison of different technologies (wind, solar, nuclear, natural gas) of unequal lifespans, initial investment, operations and maintenance, and capacities (U.S. Department of Energy). The COE model used in this study is taken from the National Renewable Energy Laboratory *Wind Turbine Design Cost and Scaling Model* study (National Renewable Energy Laboratory, 2006) and defines the cost of energy as:

$$COE = \frac{FCR*ICC+LRC}{AEP} + LLC + OM \quad (12)$$

where

FCR = fixed charge rate = .1158

ICC = initial capital cost (\$)

LRC = levelized replacement cost = $\frac{\$10.7}{kW} * PR$

LLC = land lease cost = $\frac{\$.00108}{kWh}$

OM = levelized operations and maintenance cost = $\frac{\$.007}{kWh}$

The component breakdown for the ICC is further described in APPENDIX C - INITIAL CAPITAL COST BREAKDOWN. The Wind Turbine Design Cost and Scaling Model study was published in 2002 and as such cost calculations are done in 2002 dollars. This study does not investigate the accuracy of the calculated cost of energy but uses it as a metric to identify the optimum hub height to rotor diameter ratio. This method is further described in Section 3.7 Optimization Methods.

CHAPTER 3: SIMULATION AND MODELING

The body of this thesis comes from an optimization simulation run in Microsoft Excel. This section will describe the assumptions and methods used to determine the optimum hub height to rotor diameter ratio. Rotor diameter and hub height are the two independent variables that will be used to calculate the dependent variables, PR, AEP, LF, ICC, and COE. Based on current and future wind technology predictions the maximum wind turbine rotor diameter was set at 200 m and the minimum blade length was fixed at 30 meters. The height range is also between 30 and 200 meters.

3.1 Simulation Scenario Cases

When finding the optimum hub height to rotor diameter ratio there were three scenarios that were investigated. Table 3-1 describes the variables and equations that are changed between the scenarios. The following subsections detail why the variables are changed between scenarios and how the modified cost model equations are derived.

Variable/Equation	Scenario A – Base Case	Scenario B – Modified Cost Model	Scenario C – Different Location
A	.2	.2	.4
$U(z_r) - \text{m/s}$	7.25	7.25	8.25
k	$0.27 \text{AvgWindSpeed} + 0.78$	$0.27 \text{AvgWindSpeed} + 0.78$	$0.27 \text{AvgWindSpeed} + 0.23$
Tower Mass	$0.3973 * A * h - 1414$	$0.2141h^{3.0016}$	$0.2141h^{3.0016}$
Foundation Cost	$303.24 * (h * A)^{0.4037}$	$4.8147 * (h * A)^{0.8313}$	$4.8147 * (h * A)^{0.8313}$
Transportation Cost	$(1.581 * 10^{-5}) * PR^3 - 0.0375PR^2 + 54.7PR$	$0.528603d^{2.282176} + 0.551064d^{1.951347} + 59.20251PR^{0.655811} + 0.005608h^{3.522247}$	$0.528603d^{2.282176} + 0.551064d^{1.951347} + 59.20251PR^{0.655811} + 0.005608h^{3.522247}$

Variable/Equation	Scenario A – Base Case	Scenario B – Modified Cost Model	Scenario C – Different Location
Roads & Civil Cost	$[(2.17 * 10^{-6}) * PR^2$ $- 0.0145$ $* PR$ $+ 69.54]$ $* PR$	$(-4 * 10^{-7})$ $* (PR * h)^2$ $+ 1.6227(PR * h)$ $+ 55414$	$(-4 * 10^{-7}) * (PR * h)^2$ $+ 1.6227(PR * h)$ $+ 55414$

Table 3-1. Summary of scenario variables and equations

3.1.1 Scenario A – Base Case

Scenario A is the base model which assumes that the wind turbines will be built with tubular tower sections in an open field in Oklahoma. The simulation assumes a power law coefficient of .2 with a reference wind speed of 7.25 m/s at a 30 m hub height. The simulated wind speed data is found based on the historical wind speed map of Oklahoma (National Renewable Energy Laboratory). To be more specific, the Keenan II Wind farm located in Woodward, Oklahoma was used as the geographical location of the simulated wind turbines in Scenario A and B. The power law coefficient of .2 was based off the assumption that the simulated wind turbines would be near “tall row crops, hedges and a few trees” (Ray, Rogers, & McGowan, 2006). Scenario A also follows the *WindPact Design Cost and Scaling Model* (National Renewable Energy Laboratory, 2006) with no modifications. Figure 3-1 shows the cost breakdown of the *Design Cost and Scaling Model* which when compared to Figure 3-2, the simulated model cost breakdown used in this thesis, they are almost identical. It should be noted that both models are based on a turbine with a 70 m rotor diameter with a hub height of 65 m and have a 1500 kW machine rating and all costs are based on 2002 dollars.

Component		Cost	
Initial Capital Cost		\$1,439,067.75	
Turbine Capital Cost		\$1,055,572.59	
Rotor		\$235,663.34	
	Blades	\$152,547.25	
	Hub	\$40,316.83	
	Pitch Mechanism and Bearings	\$38,485.29	
	Spinner, Nose Cone	\$4,313.96	
Nacelle		\$637,953.77	
	Low Speed Shaft	\$21,222.57	
	Bearings	\$11,953.06	
	Gearbox	\$152,441.73	
	Mech brake, HS coupling etc	\$2,983.99	
	Generator	\$97,500.00	
	Variable Speed Electronics	\$118,500.00	
	Yaw Drive and Bearing	\$19,957.23	
	Mainframe	\$114,239.99	
	Electrical Connections	\$60,000.00	
	Hydraulic Cooling System	\$18,000.00	
	Nacelle Cover	\$21,155.20	
Control Safety		\$35,000.00	
Tower		\$146,955.48	
Balance of station		\$373,749.89	
	Foundation	\$45,818.36	
	Transportation	\$51,033.75	
	Roads, Civil Work	\$79,008.75	
	Assembly and Installation	\$38,583.78	
	Electrical Interface/Connections	\$126,603.75	
	Engineering & Permits	\$32,701.50	
LRC - \$		\$16,050.00	
OM - \$		\$39,913.16	
LLC - \$		\$6,158.03	
FCR		12%	
AEP - kWh	5,701,880.00		
COE - \$/kWh	0.040		

Figure 3-2. Simulated cost breakdown sample

3.1.2 Scenario B – Modified Cost Model

Scenario B was developed because upon further investigation of the *WindPACT Design Cost and Scaling Model* it was found that most of the component equations to calculate the initial capital cost were scaled on diameter. While the final cost for the individual turbine components was accurate, the cost model simulation did not accurately reflect real world turbine hub height to rotor diameter ratios. To modify the *WindPACT* model, each of the initial capital cost components was analyzed. Of the 31 individual turbine components that make up the ICC, only 4 were found to be dependent on height and 10 were dependent on power rating. However in this simulation the power rating was a dependent variable that was found based on the USGS dataset and scaled with increasing diameter. The component

equations from the *WindPACT* model that were broken down were the Tower mass, Foundation, Transportation, and Roads & Civil cost.

In the simulation no force analysis was done on the turbine towers to confirm that they would resist overturning. It was assumed that any tower height could be appropriately constructed to prevent overturning. The base diameter of a turbine tower is sized based on the mass of the tower and mass of the turbine nacelle components to prevent buckling. In this simulation the base diameter of the different sized towers was not taken into consideration and was assumed to be constant across various heights. This assumption can lead to an overestimation of tower mass (and subsequent cost) at lower tower heights as the base diameter would be larger than needed for a lighter turbine nacelle. However the current *WindPACT* model conservatively estimates the tower mass and was not designed to accurately predict tower masses much greater than 80 meters. The simulation used in this thesis modifies the *WindPACT* model to remove the dependence of the size of the turbine nacelle (based on rotor diameter) and make it solely dependent on hub height. The same five simulated turbines in the *WindPACT* model are used to generate the new scaling equation of tower mass (Eq. 13) for Scenario B. Table 3-2 compares the Scenario A tower mass scaling equation to Scenario B's modified scaling equation for several simulated tower heights and rotor diameters.

$$Tower\ mass = 0.2141h^{3.0016} \tag{13}$$

H - m	D - m	Scenario A	Scenario B
55	55	75,752.16	35,850.01
75	65	146,194.89	90,949.55
95	85	319,142.33	184,906.36
115	85	386,776.72	328,100.81
135	105	694,524.88	530,916.85
155	105	797,731.68	803,741.31

Table 3-2. Tower mass scaling equation comparison

The *WindPACT* model assumes a Patrick and Henderson foundation type which is less common than the square pad and pier foundation. The Patrick and Henderson foundation is also only used in areas with loose soil. Therefore Scenario B assumes that the new foundation style will be the square pad and pier foundation. Data from *Design Technical Area 4 Balance of Station Cost* (National Renewable Energy Laboratory, 2001) was used to determine the foundation cost as a function of tower height and

swept rotor area, the new scaling equation is given by Equation 14. It should be noted that the *Technical Area 4* paper says that these foundation cost estimates can still be 40 – 50% conservative. Table 3-3 compares the foundation cost from Scenario A to the new scaling equation generated in Scenario B.

$$\text{Foundation cost} = 4.8147 * (h * A)^{0.8313} \quad (14)$$

D - m	H - m	Scenario A	Scenario B
50	65	\$ 34,918.52	\$ 84,555.11
85	111	\$ 66,518.74	\$ 318,776.54
120	156	\$ 100,816.03	\$ 750,496.50
170	221	\$ 153,719.83	\$ 1,788,937.32

Table 3-3. Comparison of scenario A and scenario B scaling equation.

The transportation costs given by the *WindPACT* model are only dependent on the size of the turbine. Without the tower height dependence the model would not reflect an increase in initial capital cost for increasing tower heights. Using the *Technical Area 2* (National Renewable Energy Laboratory, 2000) study the transportation cost was broken down by the blades, hubs, nacelle, and towers. It was assumed in *Technical Area 2* that all tower sections larger than the allowable 4.5 m in diameter (the maximum allowable height to be able to fit under most bridges) are pre-quartered for transportation and re-fabricated at the wind farm site. The average transportation cost for each turbine component for the five simulated turbines used in the *Technical Area 2* study are listed in Table 3-4.

Turbine Rating	Transportation Cost				
	750 kW	1500 kW	2500 kW	3500 kW	5000 kW
Blades	\$ 3,735.00	\$ 7,076.25	\$ 13,762.50	\$ 30,502.50	\$ 20,562.50
Hub	\$ 1,704.38	\$ 3,626.25	\$ 5,925.00	\$ 7,498.75	\$ 9,437.50
Nacelle	\$ 3,952.50	\$ 7,398.75	\$ 13,812.50	\$ 12,670.00	\$ 12,575.00
Tower	\$ 12,267.50	\$ 41,095.00	\$ 90,841.67	\$ 172,410.00	\$ 262,700.00

Table 3-4. Scenario B transportation cost data (National Renewable Energy Laboratory, 2000)

The data from Table 3-4 is fitted to a power trendline and summarized in Table 3-5. The independent variable 'x' for each turbine component is listed as well as the coefficient of determination for each simulated trendline.

	Trendline: ax^b			
	x	a	b	R ²
Blades	d	0.5286	2.2822	0.8788
Hub	d	0.5511	1.9513	0.9759
Nacelle	PR	59.2025	0.6558	0.8440
Tower	h	0.0056	3.5222	0.9914

Table 3-5. Scenario B transportation subcomponent trendline

To find the total transportation cost for Scenario B the sum of the individual components is added together and is presented in Equation 15.

$$\begin{aligned}
 \text{Transportation Cost} &= \text{Blades Cost} + \text{Hub Cost} + \text{Nacelle Cost} + \text{Tower Cost} \\
 \text{Transportation Cost} &= .528603 * d^{2.282176} + .55106 * d^{1.951347} + 59.20251 * PR^{.655811} \\
 &\quad + .005608 * h^{3.522247} \tag{15}
 \end{aligned}$$

Lastly the roads and civil cost was modified from the *WindPACT* model because it was only scaled on the power rating. The roads and civil cost is the cost to build any additional roadways that would be needed to transport the towers and heavy equipment between turbine towers in a wind farm that cannot be transported on the main roadways. Since tower height is an important factor in transportation between turbine sites the original cost model is modified to include height in the final calculations. To simplify the modified cost model the power rating and height were assumed to have the same magnitude of effect on the final cost. To get the modified roads and civil cost equation, the power rating and height for the five simulated turbines in the *Technical Area 4* model (Table 3-6) are multiplied together and plotted against the known roads and civil cost to get the polynomial trendline (Eq. 16).

H - m	PR - kW	Cost per turbine - \$
65	750	134,000
111	2,500	467,800
156	5,000	1,120,000
221	10,000	2,053,000

Table 3-6. Subtotal roads and civil cost breakdown for Scenario B

$$(-4 * 10^{-7}) * (PR * h)^2 + 1.6227(PR * h) + 55414 \tag{16}$$

3.1.3 Scenario C – Different Location

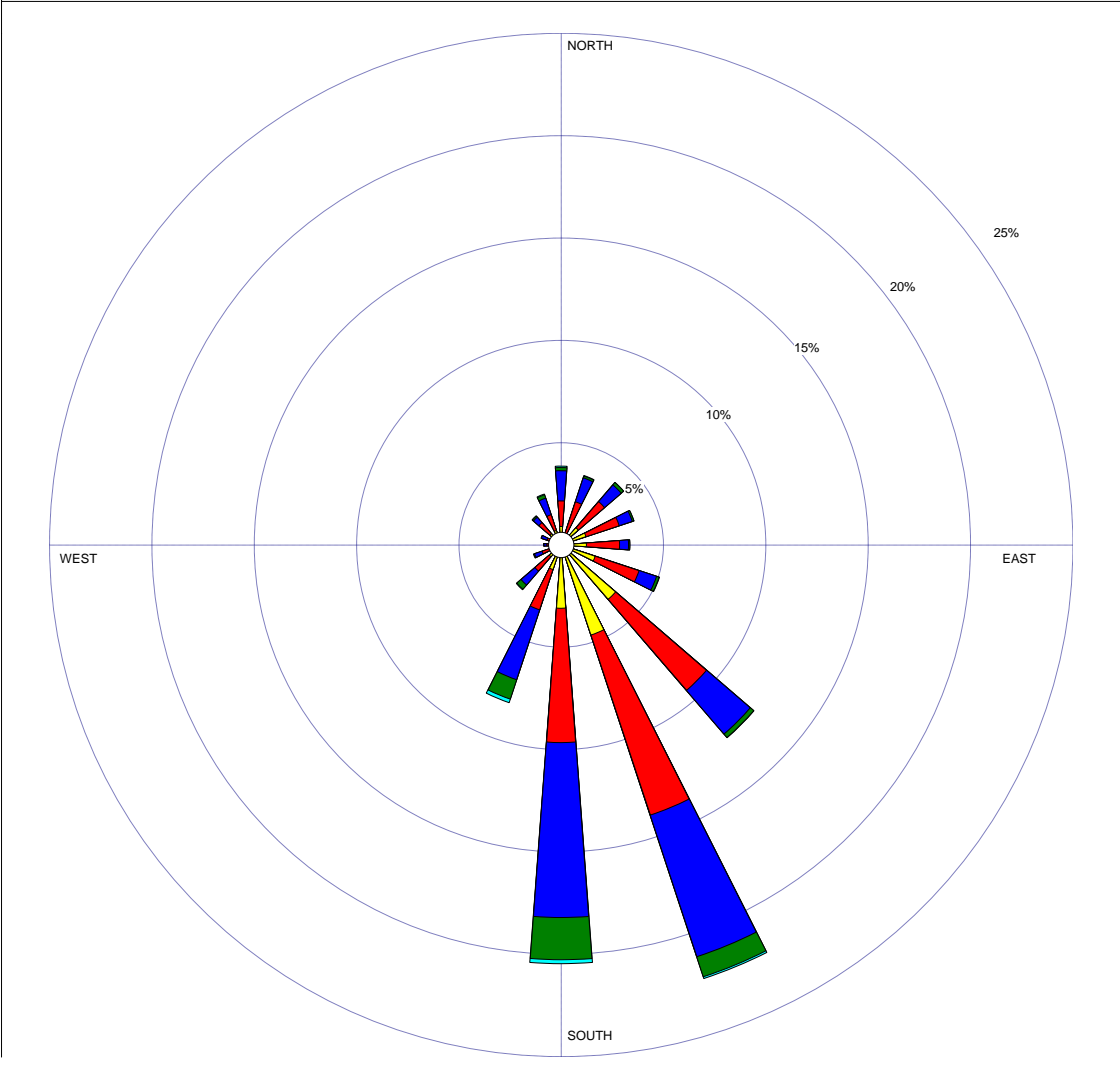
Scenario C uses the same modified cost model from Scenario B but looks at the effect of changing the theoretical geographical location on the wind turbine output. The modified cost model is used in Scenario C because Scenario B proved to have improved hub height to rotor diameter ratios. In Scenario C the new wind farm site is located at the Seven Mile Wind Farm near Rawlins in southeast Wyoming. This location was chosen because the effect of a varying surface roughness wanted to be investigated on the wind turbine output. The new reference wind speed of 8.25 m/s was found using a wind resource map of Wyoming (National Renewable Energy Laboratory). The surface roughness coefficient was estimated at .4 due to the nearby mountainous terrain (Figure 3-3).



Figure 3-3. Seven Mile Wind Farm site location for Scenario C (PacifiCorp, 2011)

Lastly a wind rose profile near Woodward, Oklahoma (Figure 3-4) taken from the USDA dataset was compared to a wind rose profile near the Wyoming site (Figure 3-5). A wind rose profile shows the direction and magnitude of the wind velocity at a particular site over a period of time. Figure 3-5 reveals a higher variation in wind direction for the Wyoming site. When analyzing wind farm sites a consistent wind speed and direction are preferred because any quick change in wind speed is power lost as the turbine has to pitch and yaw into the headwind. This is why offshore wind farms are a very desirable location because the wind speeds are very high and the wind direction can easily be predicted. For this reason, the shape parameter k for the wind profile is lowered. The shape parameter determines how consistent the wind speeds are around the predicted average. Referring to Figure 2-4, the shape parameter at 8.25 m/s was taken at the lowest point which was approximately .55 lower than the nominal value.

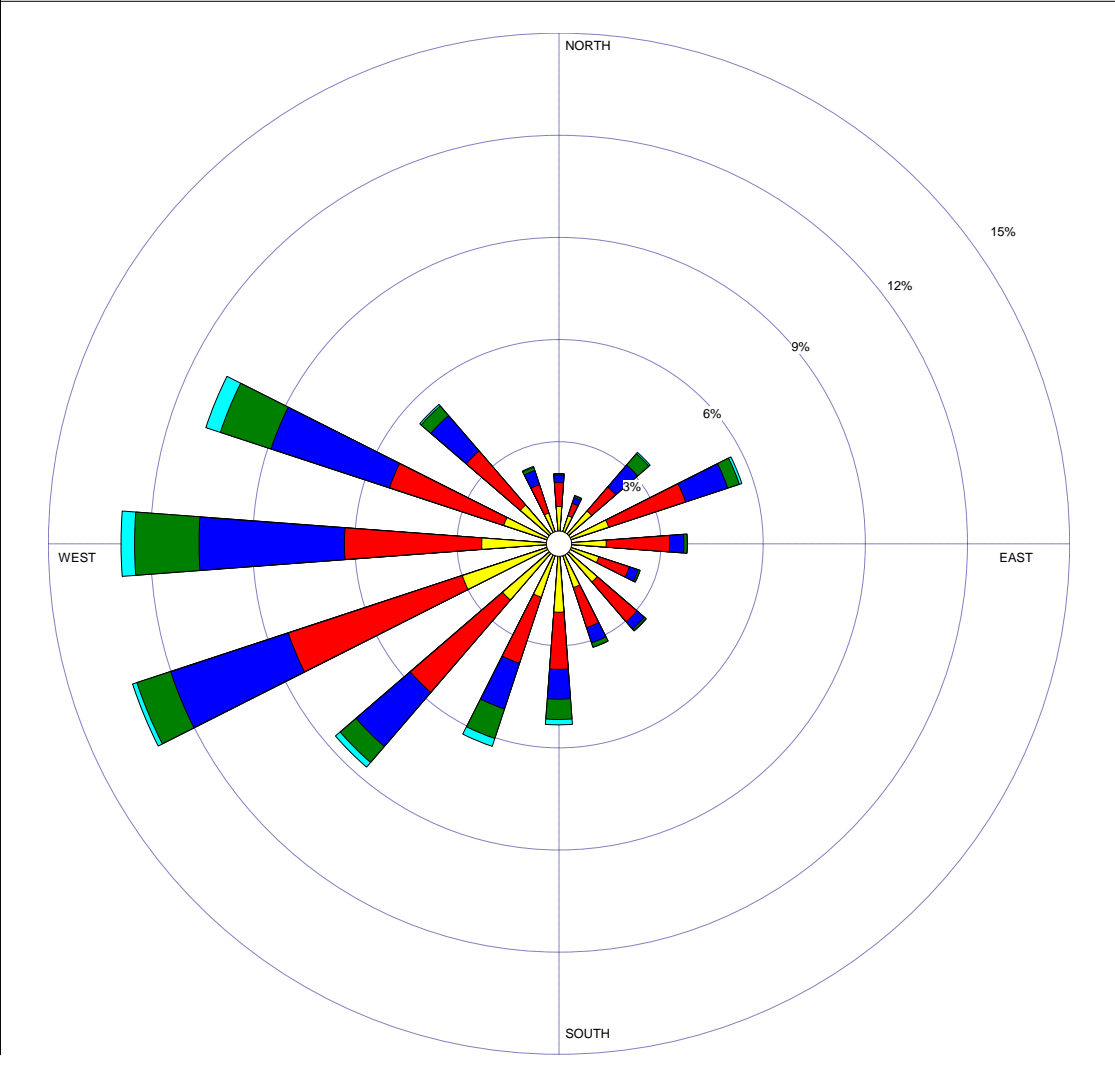
WIND ROSE PLOT
Station #13967 - OKLAHOMA CITY/WILL ROGERS WOR, OK



Wind Speed (m/s) 	MODELER Sara West	DATE 8/28/2002	COMPANY NAME USDA-ARS
	DISPLAY Wind Speed	UNIT m/s	COMMENTS
	AVG. WIND SPEED 5.07 m/s	CALM WINDS 2.31%	
	ORIENTATION Direction (blowing from)	PLOT YEAR-DATE-TIME 1961 Jun 1 - Jun 30 Midnight - 11 PM	

Figure 3-4. Oklahoma City, Oklahoma wind rose profile (National Water & Climate Center, 2002)

WIND ROSE PLOT
Station #24027 - ROCK SPRINGS/FAA AIRPORT, WY



<p>Wind Speed (m/s)</p> <ul style="list-style-type: none"> > 11.06 8.49 - 11.06 5.40 - 8.49 3.34 - 5.40 1.80 - 3.34 0.51 - 1.80 	<p>MODELER Sara West</p>	<p>DATE 9/3/2002</p>	<p>COMPANY NAME USDA-ARS</p>	
	<p>DISPLAY Wind Speed</p>	<p>UNIT m/s</p>	<p>COMMENTS</p>	
	<p>AVG. WIND SPEED 5.11 m/s</p>	<p>CALM WINDS 9.35%</p>		
	<p>ORIENTATION Direction (blowing from)</p>	<p>PLOT YEAR-DATE-TIME 1961 Jun 1 - Jun 30 Midnight - 11 PM</p>		

Figure 3-5. Rock Springs, Wyoming wind rose profile (National Water & Climate Center, 2002)

3.2 Average Power Rating

All turbines are specifically designed for the geographical location in which they will operate. As such, there can be a range of power ratings for any given height or diameter. To determine the relationship between power rating and height/diameter, Figure 3-6 and Figure 3-7 will be analyzed. Figure 3-6 shows that power rating is more closely correlated to diameter. The correlation between height and power rating was assumed to be influenced by the relationship between height and diameter shown in **Error! Reference source not found.**

Figure 3-6 and Figure 3-7 are generated from the USGS wind turbine dataset (United States Geological Survey, 2016) which is a compilation of almost 48,000 turbines within the United States. The database includes information of each turbine's location, tower height, rotor diameter, power rating, and other manufacturer's information. To reduce the number of data points that the graphs were displaying only unique data points were plotted, decreasing the number of entries from 48,000 to approximately 100 entries for each graph. Altering the dataset to only include unique points will change the final trendline and R^2 value. However, the purpose of this graph is to provide an estimation of the power rating at any given diameter - therefore the range of diameter and power ratings is more important than the magnitude of entries at each point.

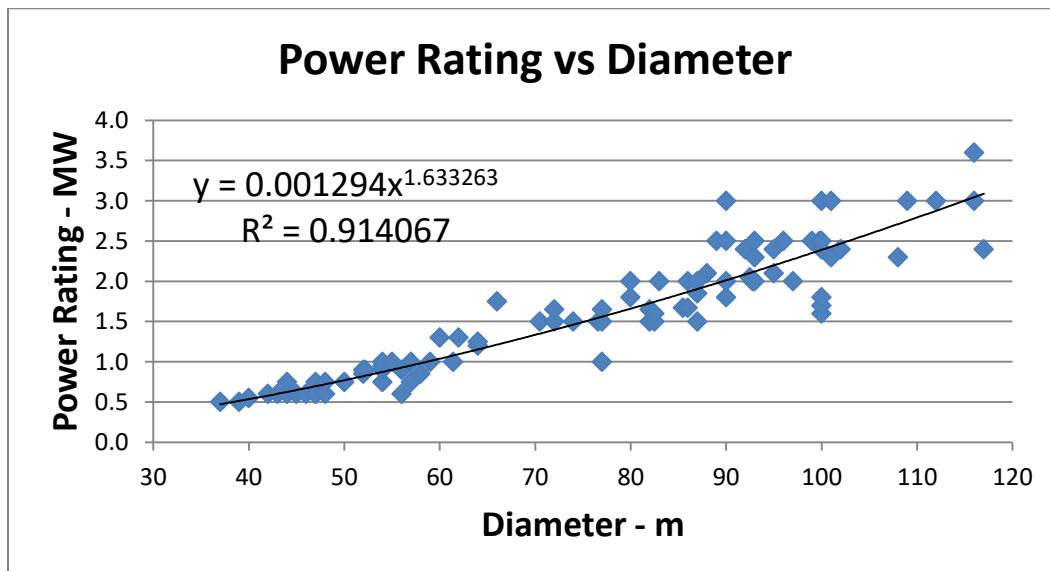


Figure 3-6. USGS Dataset Power Rating vs Diameter

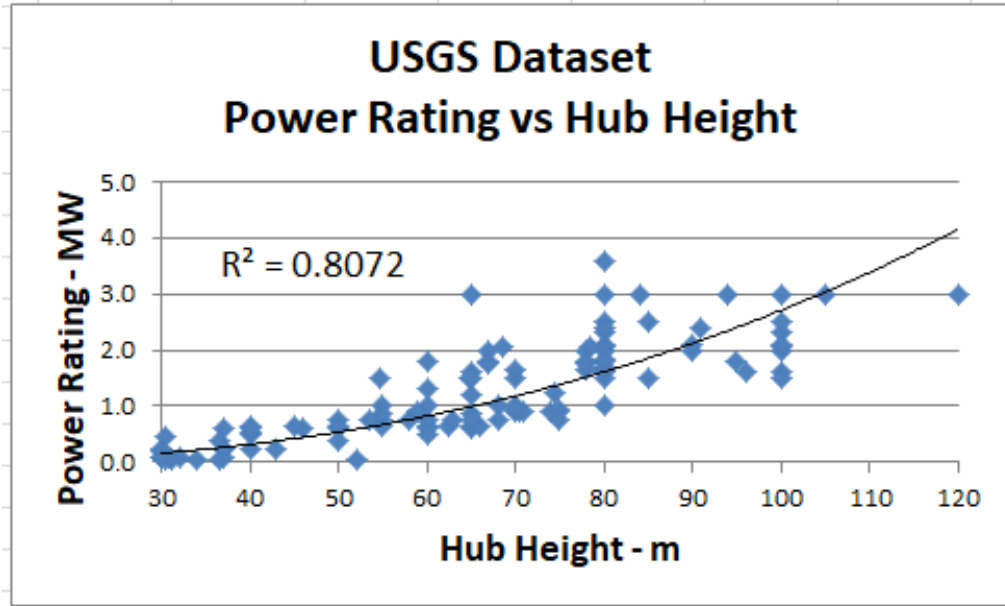


Figure 3-7. USGS Dataset Power Rating vs Height

From the trendline of Figure 3-6 the power rating in kilowatts for any given diameter in meters can be found (Eq. 18).

$$PR = (.001294 * d^{1.633263}) * 1000 \quad (17)$$

3.3 Power Curve Database

To get an estimate of the power curve for a turbine of any given diameter (since height is independent of the power curve) the power curve database from *The Wind Power* (The Wind Power) was used. This database includes information from 752 turbine manufacturers across the globe. The information provided includes each turbine name and corresponding power output for each wind speed between 0 and 35 m/s. From the turbine name the rotor diameter and rated power can be found and it was added to the dataset for analysis purposes.

Before analysis was done in the simulation the effect of varying diameter and power rating on the turbine power curve was investigated. Figure 3-8 shows all the power curves for each 1000kW turbine in the power curve database. As expected the slope of the power curve increased with increasing rotor diameter. It can be concluded that as the rotor diameter increases the power output of the turbine increases proportionally to the square of the rotor diameter (referring to Equation 8). Figure 3-9 summarizes the relationship of a constant rated power and increasing rotor diameter.

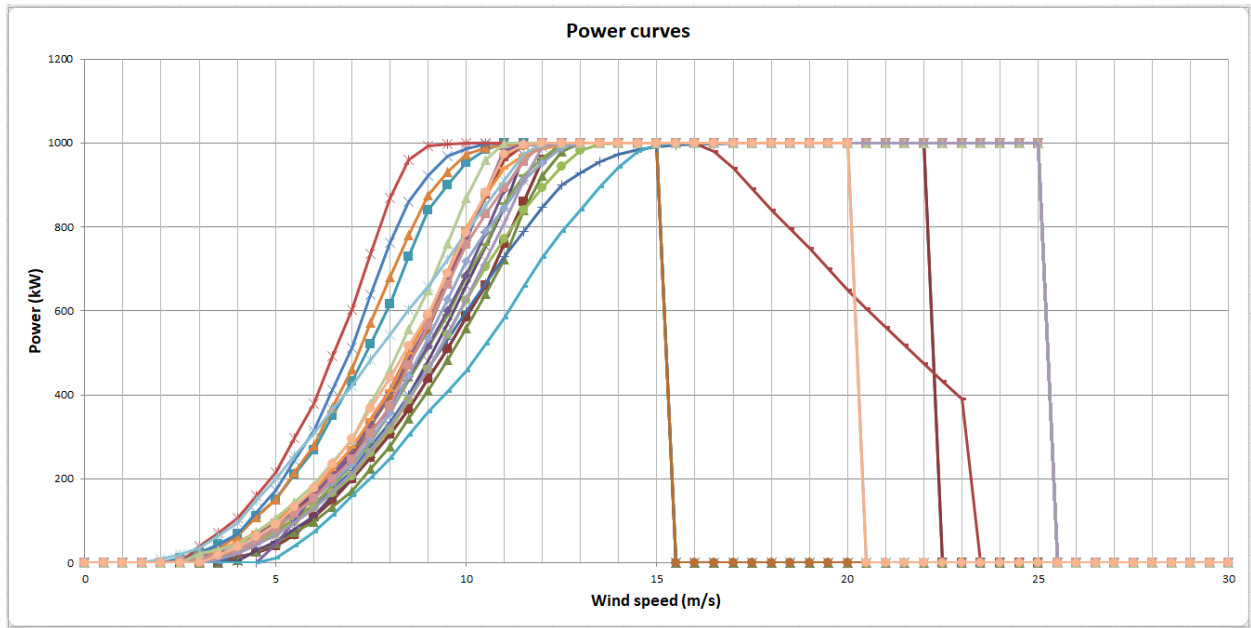


Figure 3-8. Power curves for all turbines at 1000kW

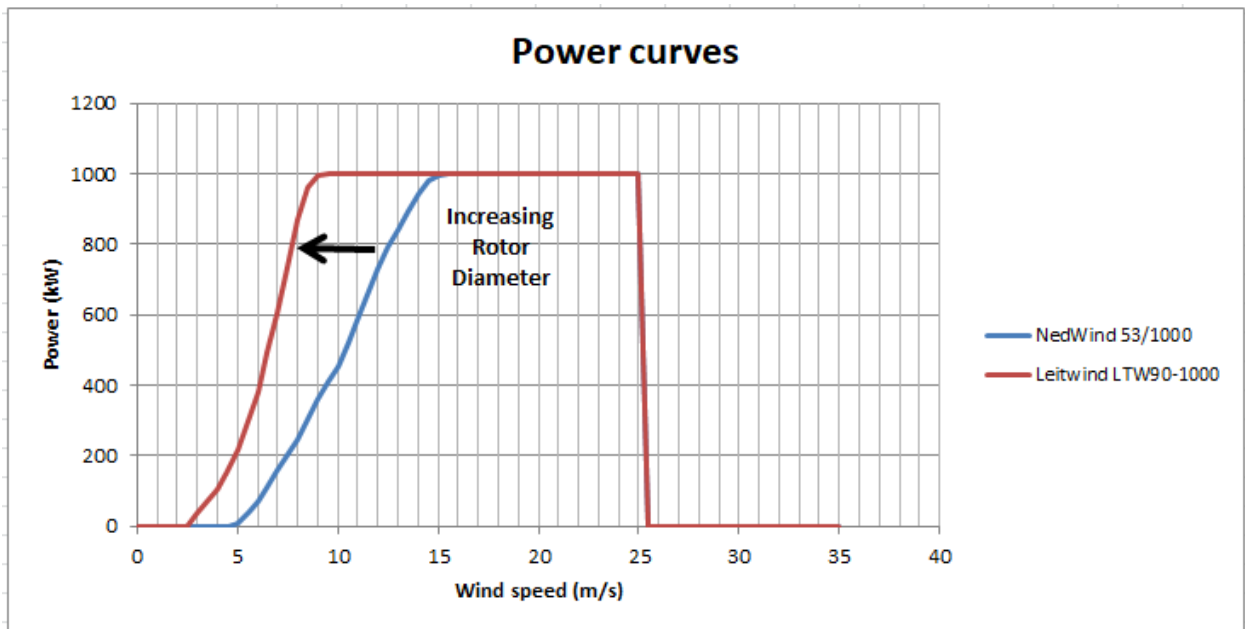


Figure 3-9. Power curve relationship for increasing rotor diameter at constant power rating

Next the effect of varying the power rating of the turbine at a constant diameter was investigated.

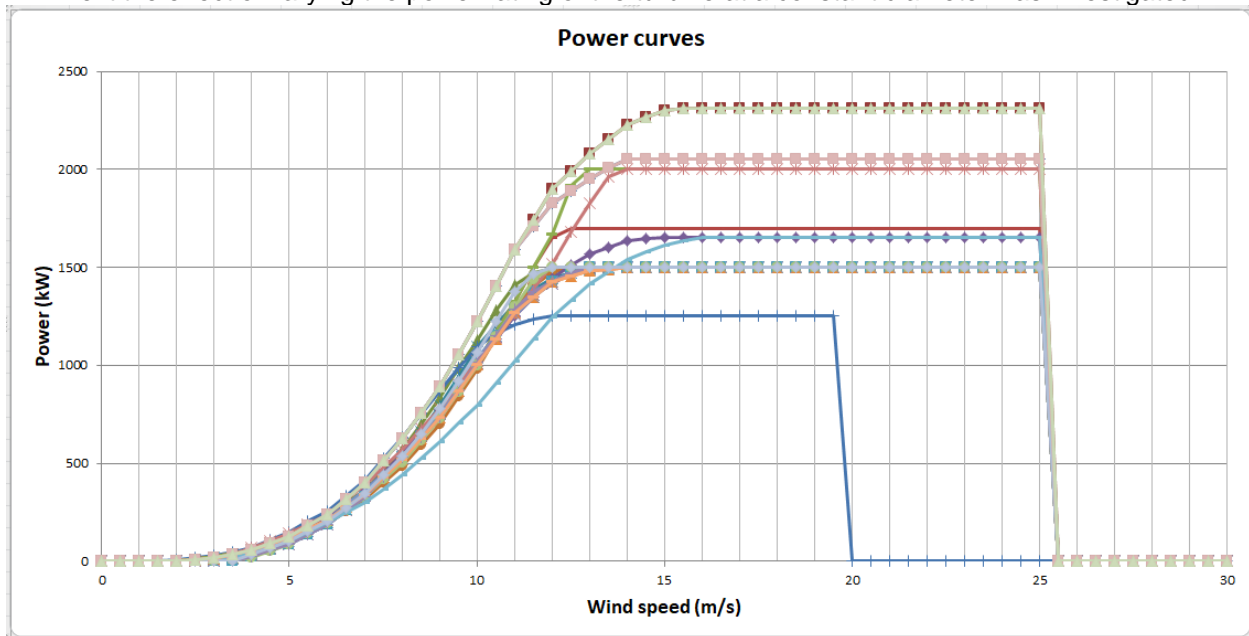


Figure 3-10 shows the power curves of all 70m blades in the power curve database. Every power curve within this range has approximately the same slope. Figure 3-11 summarizes the range of power curve slopes for a 70 m rotor diameter. The maximum percent difference between the average and the max value was 23% and the percent difference between the average and the minimum value was 18%. It can be concluded that since the max and min are within approximately one standard deviation of the average that the slope of the power curve is independent of power rating.

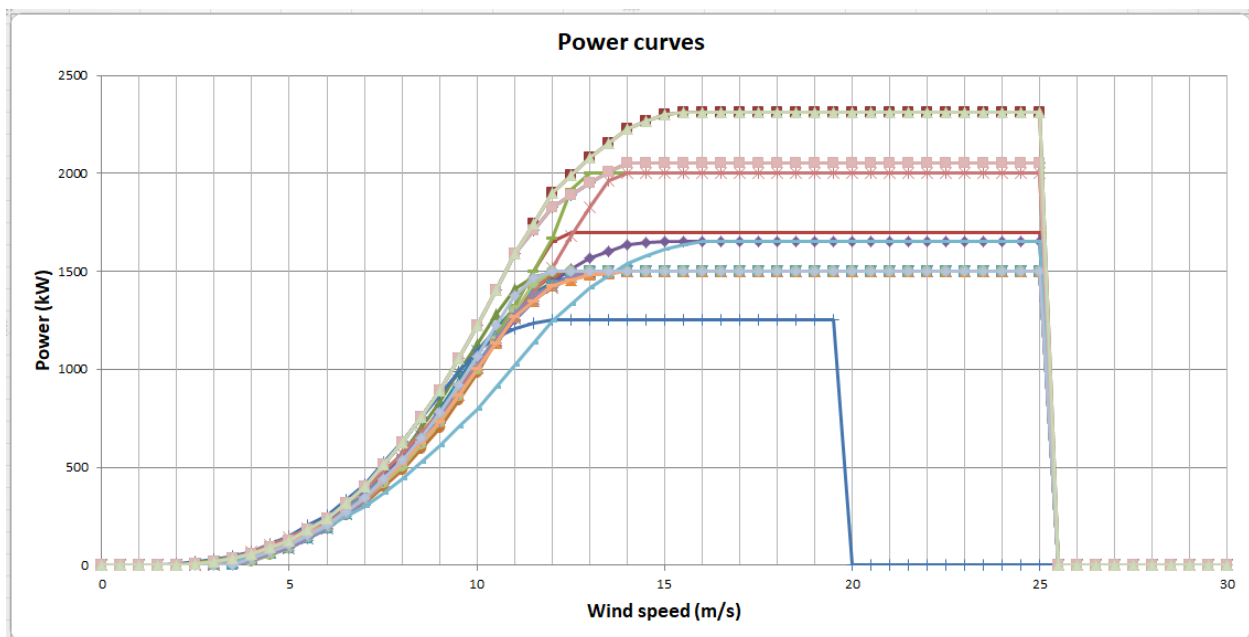


Figure 3-10. Power curves for all turbines with 70 m rotor diameter

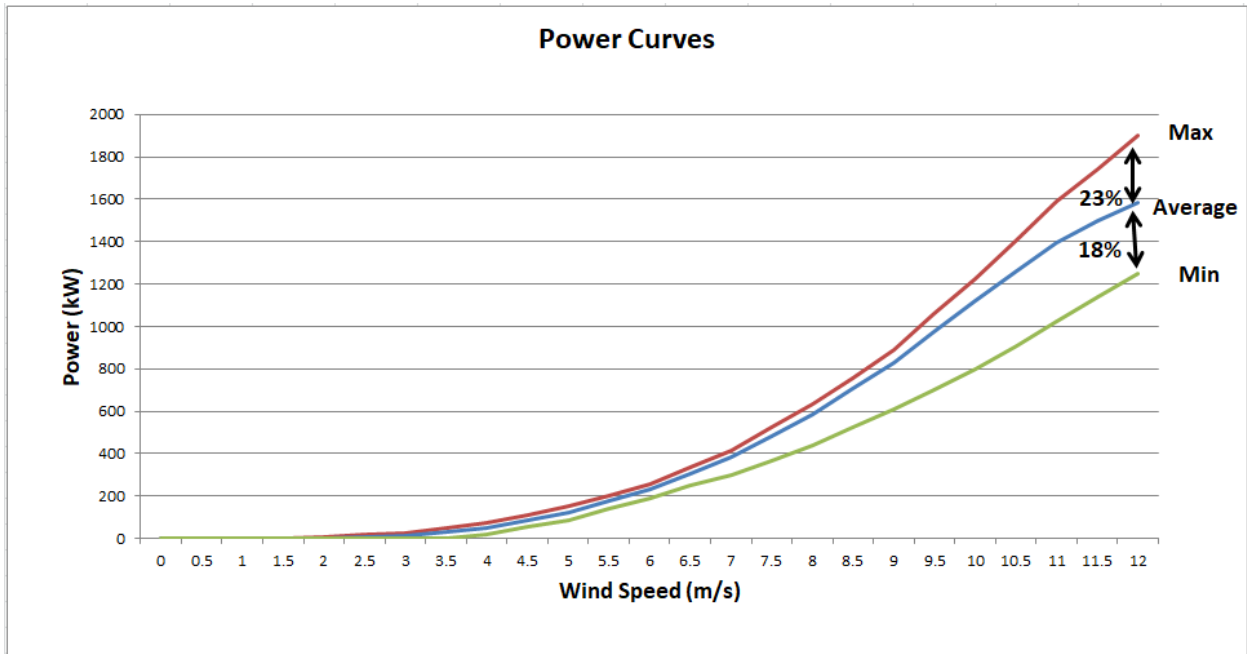


Figure 3-11. Power curve range for 70 m rotor diameter

With these trends in mind the original power curve database had to be expanded. In order to accurately predict the energy production of a wind turbine, a power curve is needed - however the original power curve database does not include a power curve for every rotor diameter size. Based on Figure 3-10 and Figure 3-11, an average slope of the power curve can be found for any given diameter which will accurately predict the power output of a turbine. For every rotor diameter between 30 and 200 meters the average power curve slope was calculated and the missing rotor diameter slopes were interpolated between points. Table 3-7 shows a sample of the power curve trendline dataset where the red lines are the missing diameters and values for a and b are interpolated between the closest known data points. All power curve trendlines are based on the generic power trendline equation (Eq. 18). APPENDIX B - Power Curve Trendline Data gives a complete table of the wind turbine power curve trendline dataset.

$$P(v) = a * v^b \quad (18)$$

where

$P(v)$ = power output (kW)

v = wind speed (m/s)

Diameter	a	b	R ²
60	1.0813	2.7705	0.9783

61	1.4319	2.6501	0.9681
62	0.8574	2.8806	0.9681
63	0.8530	2.9076	0.9723
64	0.7268	3.0211	0.9827
65	0.2540	3.5076	0.9896
66	1.3020	2.7599	0.9582
67	1.1276	2.8511	0.9669
68	1.1047	2.8743	0.9696
69	0.9534	2.9669	0.9770
70	0.8243	3.0587	0.9834

Table 3-7. Power curve trendline sample dataset

Within the power curve database the cut in, cut out, and rated speed of each turbine was given. Analysis was done on each of these values to determine if they scaled with rotor diameter or power rating. It was found that the cut in, cut out, and rated speed are all independent of rotor diameter and power rating (APPENDIX A – Cut in, Cut out, and Rated Speed relationships). Therefore for each turbine the cut in and cut out speed was kept constant. The cut in and cut out speed was found by averaging all turbine cut in and cut out speeds:

Cut in speed: 3.5 m/s

Cut out speed: 24 m/s

When comparing the simulated power curve to the Suzlon S60/1000 turbine's power curve (Figure 3-12), the model is able to accurately predict a power output that matches a real power curve. The Suzlon has a rotor diameter of 60 m, a hub height of 65 m, and a rated power of 1000 kW, the model was designed to match these parameters. The only deviation would be at the transition region around 12 m/s. At this wind speed the Suzlon turbine is pitching the blades out of the wind to reduce the power output as it approaches the generator capacity. The model assumes a perfect control system where the output of the turbine is allowed to increase until it reaches the rated power. This means that the model will always over predict the power output at the transition region. However, when comparing the model to the Suzlon turbine the model over estimates the power output by only 1.2%.

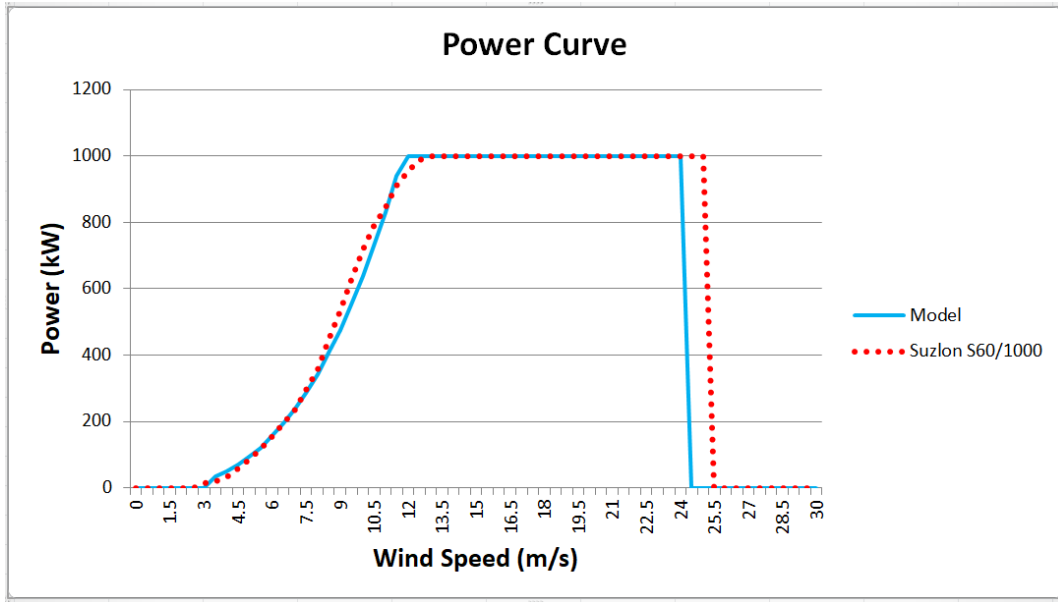


Figure 3-12. Model Validation using Suzlon S60/1000 power curve

3.4 Wind Model

Figure 3-13 shows the spreadsheet used to determine the Weibull wind speed distribution plot.

Column B is later used to find the annual energy production according to Equation 10.

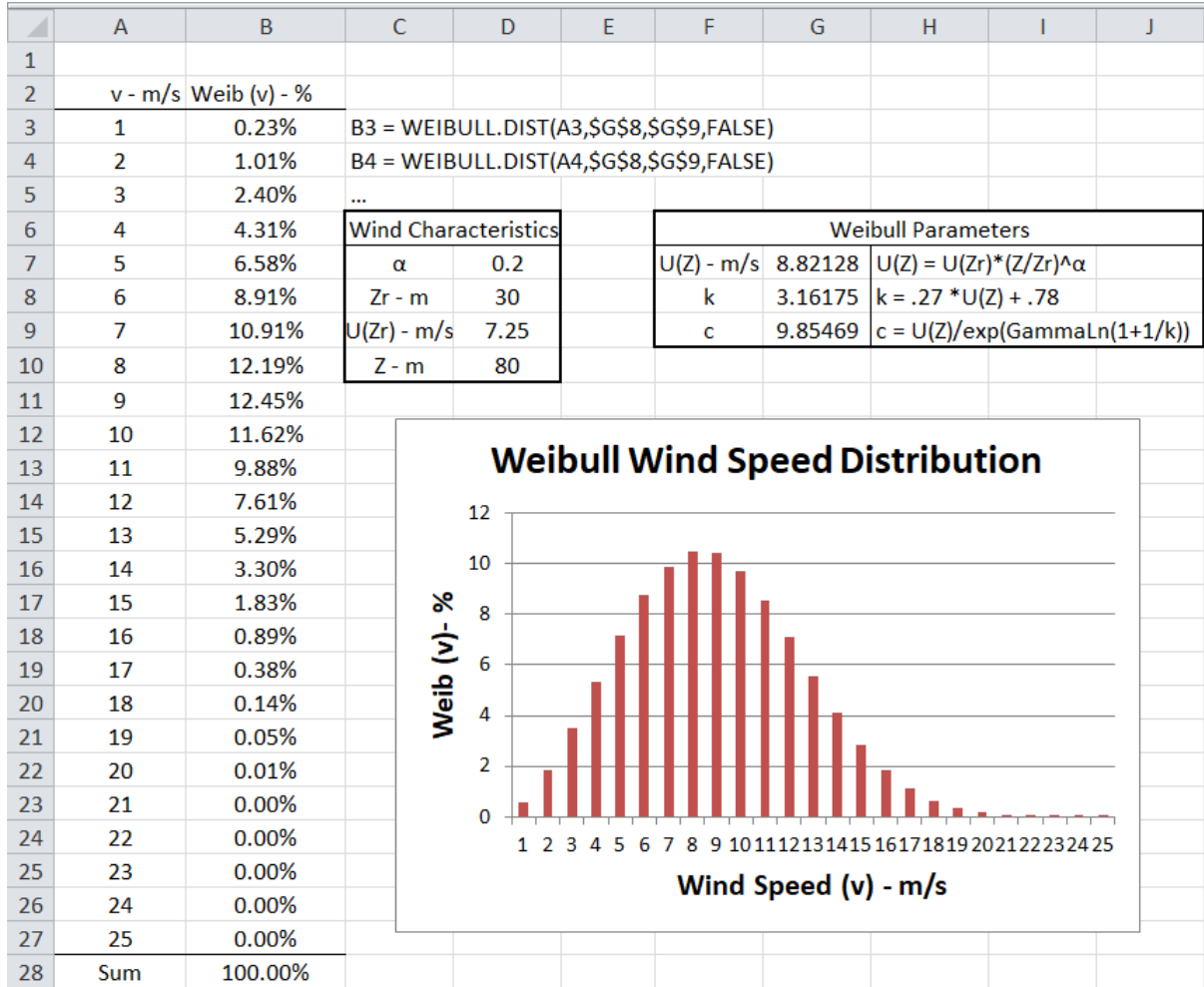


Figure 3-13. Weibull distribution calculation spreadsheet

3.5 Annual Energy Production

To determine the annual energy production of a turbine AEP was calculated for every height and diameter combination. Figure 3-14 shows an example of the AEP trends for Scenario A – Base Case.

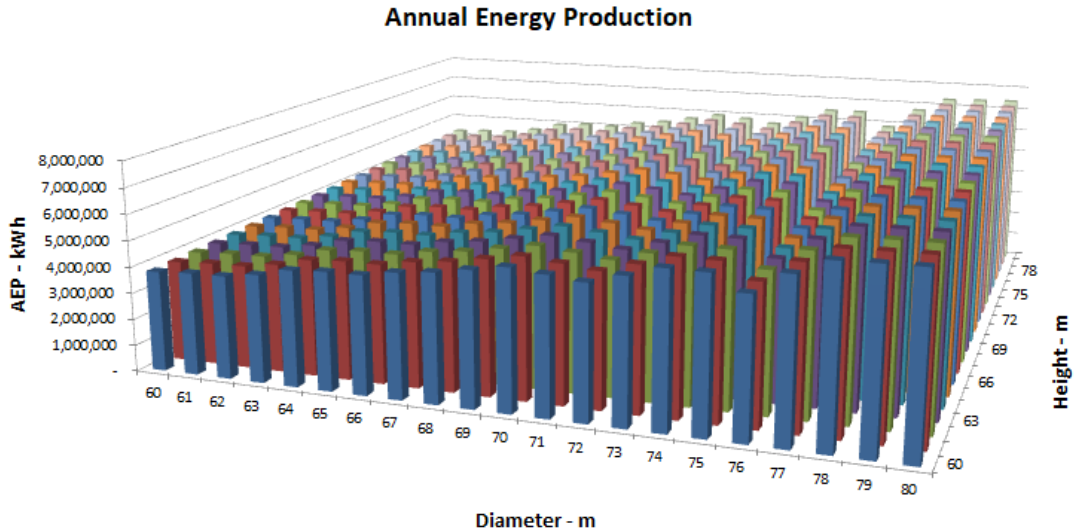


Figure 3-14. Annual energy production trends

Figure 3-14 shows that AEP is more strongly correlated to increasing diameter than increasing height. Within this particular range of data, the AEP increased on average 33,018 kWh per additional meter in height whereas the AEP increased 144,592 kWh per additional meter in diameter.

It should be noted that within the AEP calculations there were local maxima and minima between diameter sizes as shown in Figure 3-15. The AEP is calculated using the power curves generated from the power curve database. More power curve data for each diameter within the range would help to reduce these local maxims to fit general power curve trends.

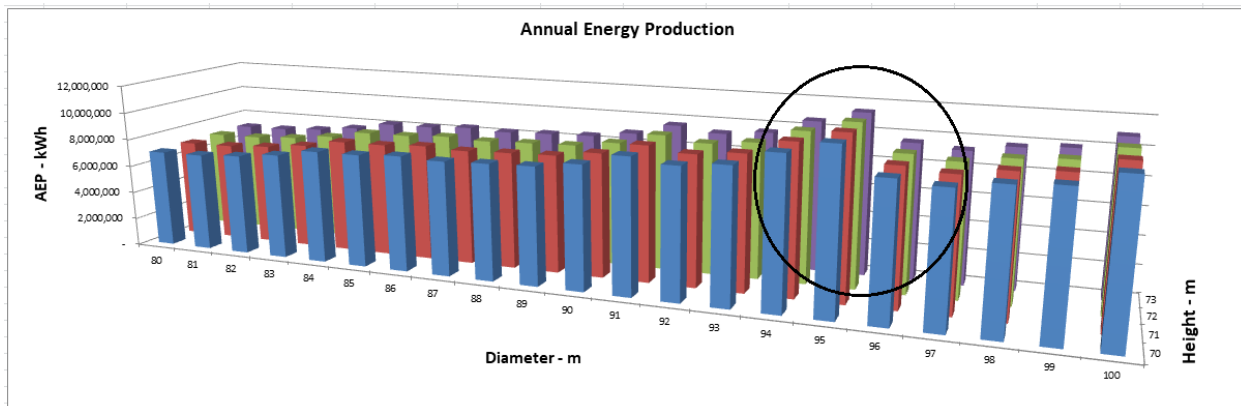


Figure 3-15. AEP local maxima

3.6 Load Factor

Figure 3-16 shows the common trend for the Load Factor across different diameter and height combinations. Similar to the AEP trend, the load factor was found to have slight fluctuations between different diameters which was attributed to a lack of data. However on average the load factor did increase with increasing diameter. When looking at increasing height, the load factor increased consistently. Since the general trend of the load factor for both diameter and height increased, this means that any increase in height or diameter will provide an inherently more efficient turbine.

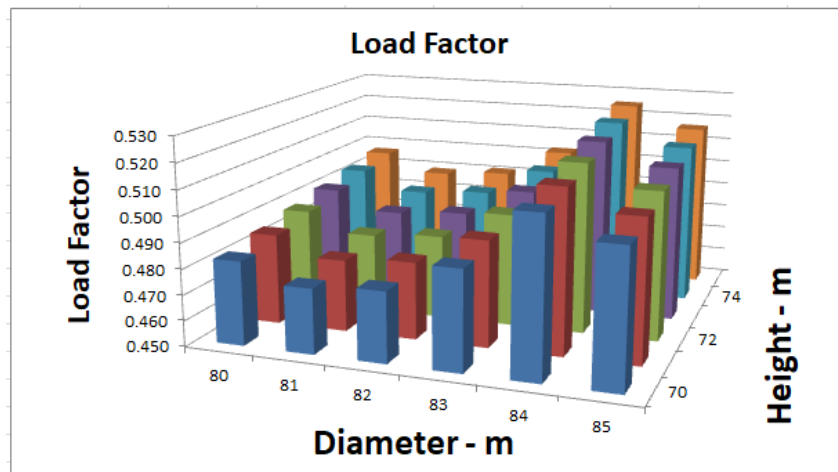


Figure 3-16. Load factor trends

3.7 Optimization Methods

The main optimization method used was the COE method; the COE/LF method was an extension of the first method to attempt to include the turbine efficiency in the final optimum hub height to rotor diameter ratio. The goal of the COE model is to minimize the cost of energy to predict the height and diameter that has the cheapest initial capital cost and the highest annual energy production. Similarly the COE/LF method minimizes the COE/LF ratio to find the hub height and rotor diameter with the cheapest cost of energy and the highest load factor. APPENDIX D – COE/LF SIMULATION FLOWCHART describes the COE/LF optimization method flow chart for finding the optimum height given a certain diameter.

Figure 3-17 shows a sample graph of cost of energy plotted against a varying height at a constant diameter of 70 m. The minimum value of COE corresponds to a height of 69 m for the 70 m rotor diameter turbine.

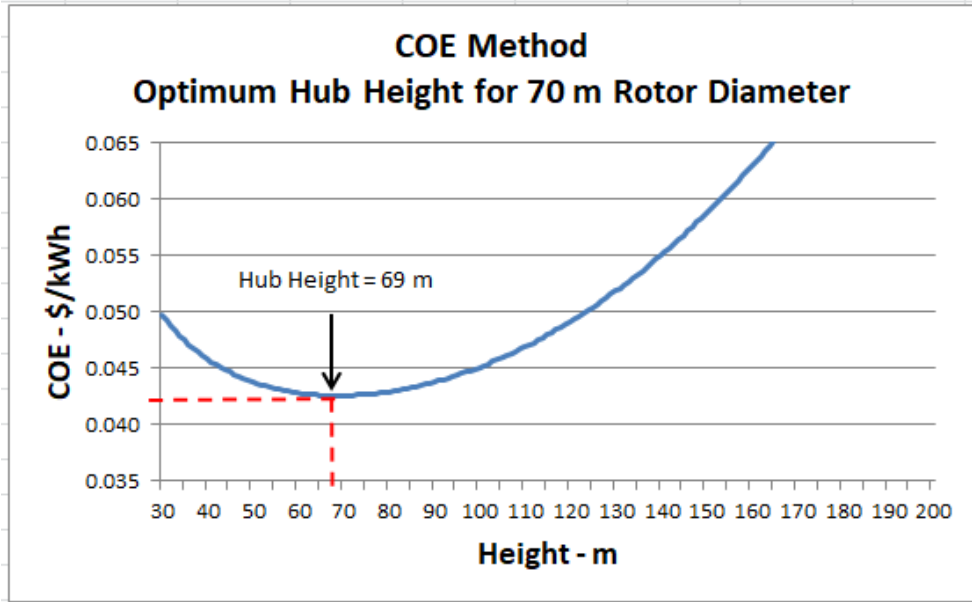


Figure 3-17. COE optimization method sample graph

Figure 3-18 shows the same graph of AEP and ICC but instead plotted against a varying *diameter* at a constant height of 70 m. Due to the slight variation in power curves between blade sizes, local maxima and minima exist within the AEP dataset (Figure 3-15). If no trendline were used then the optimum diameter would be 95 m, yet when a polynomial trendline is used the optimum diameter is found to be 131 m. Therefore in all COE and COE/LF simulations when determining the diameter at a given height, a polynomial trendline is used to more accurately predict the optimum hub height to rotor diameter ratio.

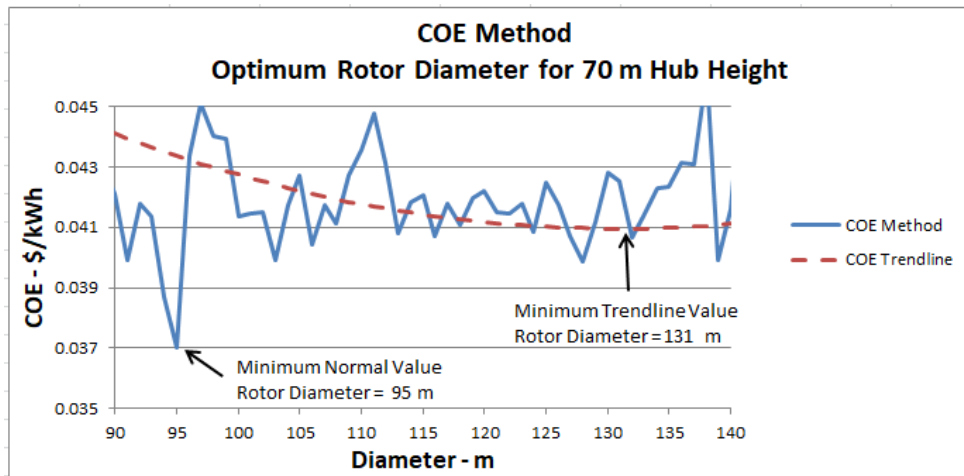


Figure 3-18. COE optimization method at constant height

Following the same procedure, a sample graph of the COE/LF optimization method is shown in Figure 3-19 below.

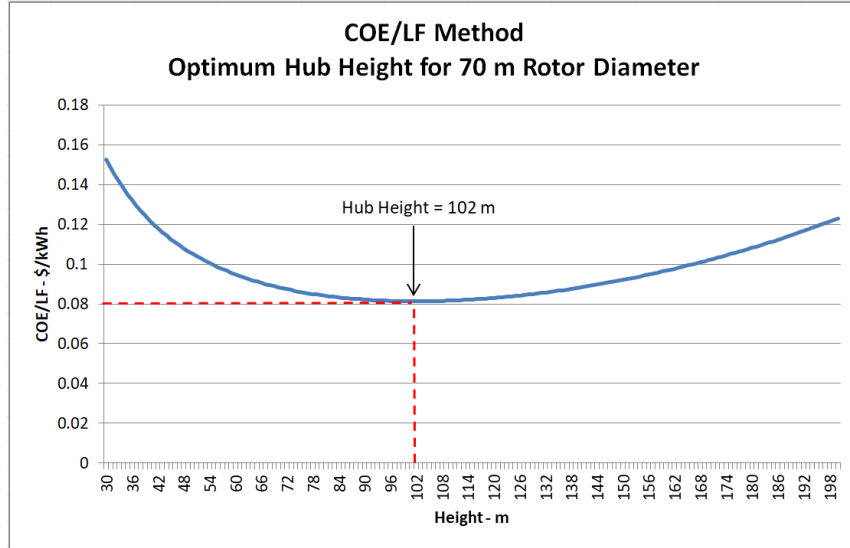


Figure 3-19. COE/LF optimization method sample graph

Using the calculated values of COE, LF, ICC, and AEP the optimum hub height and rotor diameter ratios will be investigated and compared to the USGS dataset.

CHAPTER 4: DATA, ANALYSIS, AND RESULTS

This section will detail the behavior of each of the independent variables AEP, ICC, LF, and COE in each of the scenarios. Additionally the accuracy of the COE and COE/LF methods will be compared.

Table 4-1 describes how much each independent variable changes per one meter in diameter or height for each of the scenarios. For example, the initial capital cost for Scenario A is expected to increase \$10,274 for every additional meter above 30 meters. A negative value for any of the coefficients would imply that the variable decreases with increasing diameter or height.

	Scenario A		Scenario B		Scenario C	
	Diameter	Height	Diameter	Height	Diameter	Height
AEP - kWh	245,643	59,950	245,643	59,950	318,085	63,418
ICC - \$	91,829	10,274	69,989	28,460	69,989	28,460
LF	0.0021	0.0014	0.0021	0.0014	0.0024	0.0008
COE - ¢/kWh	-0.006	0.009	0.018	-0.023	0.014	-0.010

Table 4-1. Summary sheet

After analyzing preliminary results, the optimum rotor diameter for a given height did not provide accurate height to diameter ratios. Figure 4-1 shows the values obtained from the optimization simulation for Scenario A and Scenario B for diameter given height, it is for this reason the optimum rotor diameter for a specified hub height was not used in the final analysis of the report. Instead for all simulations the optimum *hub height* for a given *diameter* is the preferred method. Note that the height is on the x-axis and diameter is on the y-axis for this figure to better see the trend in diameter across the entire height range.

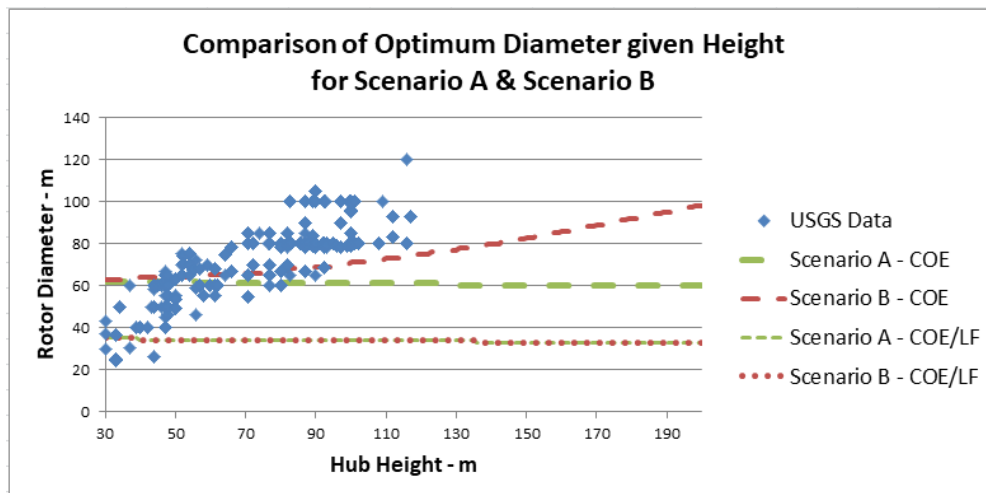


Figure 4-1. Optimum diameter given height method

Scenario B was used to compare the COE and COE/LF methods to the USGS dataset. The trendline of the USGS dataset was used to calculate the percent error in hub height for each rotor diameter. The results are summarized in Table 4-2, it was found that the COE method was more accurate at predicting the actual hub height for any given rotor diameter.

	% Error
COE	13.66%
COE/LF	37.72%

Table 4-2. Percent error between optimization methods and USGS dataset

4.1 Scenario A – Base Case

In this scenario the COE/LF method erroneously predicted the optimum hub height for every diameter to be 200 meters. Similarly, the COE optimization method consistently selected hub heights around 170 m (Figure 4-2). In the base case the estimated cost per additional meter in tower height was so cheap that it was always economical to build a taller tower. This cost model does not accurately reflect real world aspect ratios as no utility scale wind turbines are constructed at such high aspect ratios.

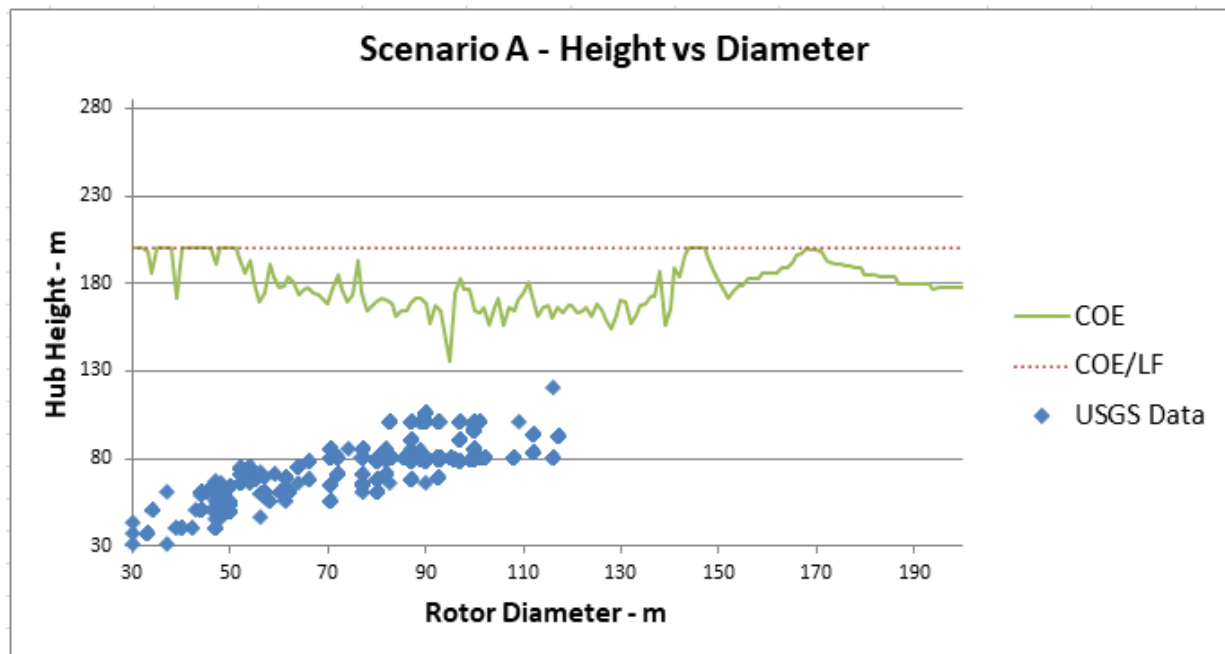


Figure 4-2. Scenario A optimum height vs diameter

4.2 Scenario B – Modified Cost Model

Figure 4-4 shows how the modified cost model influenced the total cost breakdown of the turbine when compared to the original cost breakdown (Figure 4-3) of a turbine with the following characteristics:

$$d = 88 \text{ m}$$

$$h = 75 \text{ m}$$

$$PR = 1932 \text{ kW}$$

The biggest changes were increasing the balance of station cost through the foundation and roads and civil cost. These costs were originally not scaled on height and this new model reflects an increase in cost with increasing tower height. The new cost model also shows similar cost breakdown percentages when compared to other economic analysis models (International Renewable Energy Agency, 2012)

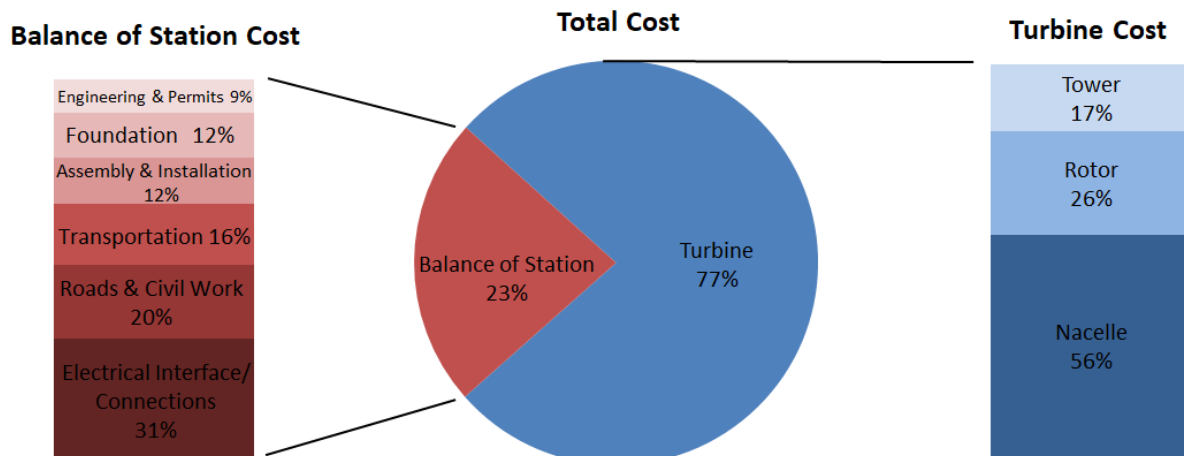


Figure 4-3. Scenario A – Cost breakdown

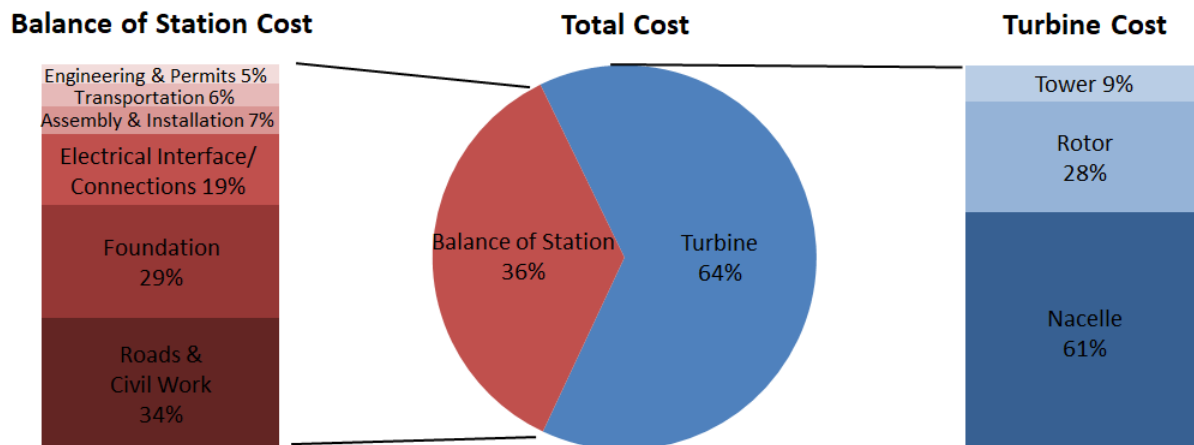


Figure 4-4. Scenario B – Cost breakdown

Figure 4-5 shows predicted optimum hub height and rotor diameters from Scenario B for the COE and COE/LF optimization methods. The COE/LF method follows the same optimum hub height trends as the COE method but consistently predicts the hub height 1.5 times higher than the COE method. When comparing the COE method to the trendline of the USGS data, the COE method has a 24% lower percent error than the COE/LF method (Table 4-2). The COE method is able to accurately predict realistic turbine heights up until 115 meters in rotor diameter. Above this value the amount of turbines significantly drops as there are not many turbines with blades above 120 meters in diameter in operation. Assuming the COE model can accurately predict wind turbine upscaling trends, future wind turbine aspect ratios would begin to approach .5 as they reach 200 m in diameter.

When comparing the COE and COE/LF optimization methods to previous optimization reports, the COE method more accurately predicts the optimum hub height (Figure 4-6). However the COE method overestimates the hub height for smaller turbines less than 70 meters in diameter. When comparing to previous optimization reports, the COE method is projected to underestimate the actual hub height for every rotor diameter above 200 meters (Figure 4-6). It is speculated that the scope of this optimization thesis is not broad enough and that there are other outside factors that are influencing the final hub height in existing turbines. As with any large scale project there are design tradeoffs that must be made to find a balance between all the interacting components. For example a choice made to lower the tower height to satisfy the static loading conditions could cause the tower to be much lower than the optimal height. In order to understand the complex interactions between turbine components, comprehensive modeling software is used to predict wind turbine behavior. Studies have been done (Ashuri, 2016) to attempt to take into consideration all the individual component software, but research in this area is still in development and more integrated software for turbine design analysis is still needed.

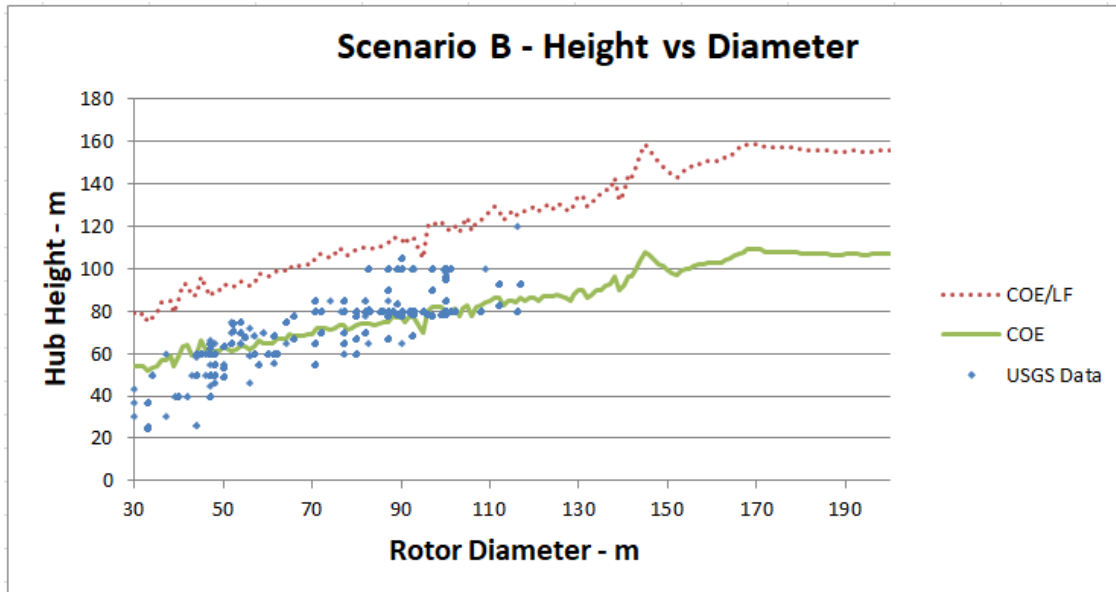


Figure 4-5. Scenario B height vs diameter

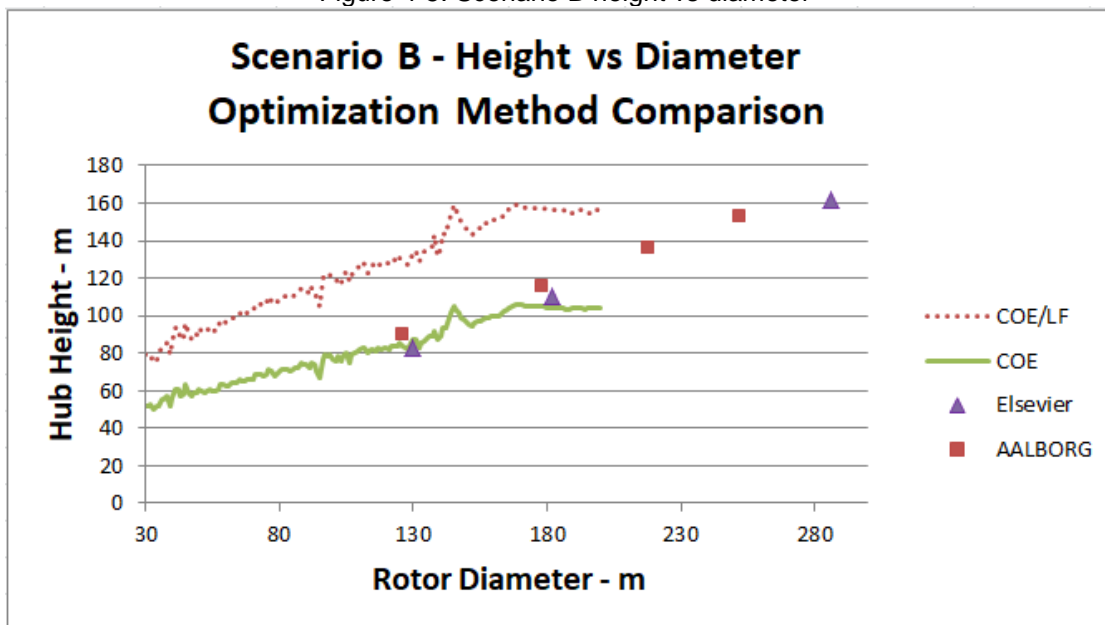


Figure 4-6. Scenario B height vs diameter of all optimization methods

4.3 Scenario C – Different Location

The biggest finding from Scenario C was that the geographical location of the wind farm highly influenced the annual energy production. By increasing the reference wind speed and power law coefficient from Scenario A and B, the AEP per unit in blade diameter increased by almost 30% and the AEP per unit in hub height increased almost 6% (Table 4-1). With such high AEP improvements a wind turbine in a mountainous region can be built at lower heights and produce the same - if not more - power than a similarly sized turbine in the plains of Oklahoma. Figure 4-7 shows how the improved AEP output

affected the optimum height vs diameter ratio across the range of diameters. At larger rotor diameters, the tower height is much lower than the simulated turbines from Scenario B – Modified Cost Model.

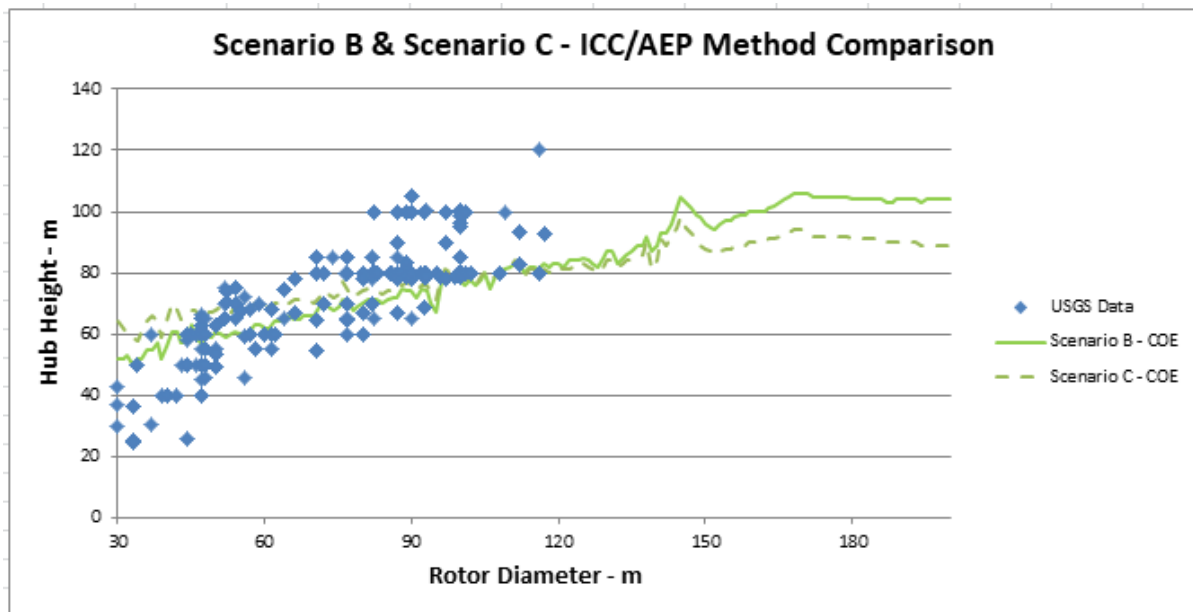


Figure 4-7. Scenario B and Scenario C height vs optimum diameter comparison

Yet despite the apparent advantages, the biggest disadvantages of siting a wind farm in a more mountainous region are the gusty and highly variable wind speeds. These high wind loads put additional stresses on turbine towers and blades and can reduce the lifespan of the turbine. Ideal wind conditions for a turbine are strong, consistent winds. This allows turbines to operate efficiently with little to no power loss with changing wind direction and reduced operation and maintenance cost.

4.4 Turbine Tower Height Limitations

This thesis assumes that the turbine tower will be made from tubular tower sections. Realistically it is not economical to build a 200 m tubular tower because current crane technology is only able to reach up to 150 meters. It is possible to build taller turbine towers but expensive crane towers must be used. The current simulation takes into consideration this increase in cost at taller tower heights and is still valid. However, other more economical options exist to construct very tall turbine towers. The first alternative is to build a hybrid concrete-tubular tower which can withstand the high static loads and help reduce the size of the tubular tower base sections which were running to physical limits in manufacturing and transportation.

CHAPTER 5: CONCLUSIONS

The main objective of this thesis was to investigate the relationship between tower hub height and blade rotor diameter. Using the power curve database from *The Wind Power*, the annual energy production and load factor of any size turbine was predicted. The *WindPACT Design Cost and Scaling Model* was used to estimate the cost of energy for the simulated turbines. Using Excel, the optimum COE was found for every diameter and the corresponding height was plotted to reveal the hub height to rotor diameter relationship. This relationship was then compared to the USGS wind turbine database to validate the simulation results.

One significant finding from this research is that the *WindPACT Design Cost and Scaling Model* cannot be used in its current state to predict the optimum hub height to rotor diameter ratio. The *WindPACT* model was designed to scale primarily on rotor diameter and to provide conservative cost estimations of various wind turbine subcomponents. However the results from Scenario B - Modified Cost Model reveal that the *WindPACT* model can be modified to more accurately reflect changes in tower height on the overall cost of the turbine.

The COE optimization model from Scenario B provided the most accurate estimate of the optimum hub height to rotor diameter ratio when compared to the USGS dataset. This model predicts that future large scale turbines nearing 200 m in diameter will have an aspect ratio closer to .5. Other notable optimization reports propose that large scale wind turbines will have a hub height to rotor diameter ratio closer to 0.7.

Scenario C suggests that the optimum wind turbine aspect ratio is dependent on geological location. Every new wind turbine must consider the surface roughness, turbulence intensity, average wind speed, and wind direction of the surrounding area. All turbines must be designed based on the location in which they will be built in order to ensure the optimum hub height and rotor diameter ratio is utilized.

CHAPTER 6: RECOMMENDATIONS FOR FUTURE WORK

The largest potential improvement that can be done is to utilize and integrate more accurate programs. Advanced software for predicting wind turbine behavior and complex wind shear models should be used to more accurately predict the optimum hub height to rotor diameter ratio.

Currently the NREL has released open source software called WISDEM which integrates many individual wind turbine models to help determine the overall wind plant cost of energy. The WISDEM software uses additional cost models besides the *WindPACT Wind Turbine Design Cost and Scaling model*. The first is a mass-to-cost model that takes individual component masses as inputs to estimate each component costs. The second is an updated version of NREL's turbine cost and sizing tool that uses data for component sizes and costs from the year 2015. The WISDEM software also includes physical analysis of the tower and nacelle components that can be used to determine the feasibility of the particular sized components. Other software that can be integrated into this simulation would be more advanced wind shear models that are able to account for the diurnal behavior of the wind shear coefficient and accurately predict the effect of varying turbulence levels on the power output of a turbine. These newer cost and physical verification models can be used to predict the optimum hub height to rotor diameter ratio to a higher degree of accuracy.

Another area for improvement that can be done with this research is to perform a sensitivity analysis on the output variables ICC, AEP, COE, and LF. This thesis only analyzed the effect of varying the height and diameter on the output variables. However, the sensitivity of many other variables was not considered. These other design variables include the wind shear coefficient, reference height and wind speed, shape parameter, scale factor, and power rating. Each of the listed variables could easily fall within a range of possible values for any particular turbine but this thesis assumed a single value for each and did not look at how much each affected the output variables.

CHAPTER 7: REFLECTIONS

By pursuing this research I have expanded my knowledge about the wind energy industry. I have learned about the various subcomponents of a wind turbine as well as the basic design parameters and cost models needed to optimize a theoretical turbine. I can see how a change in one design variable will affect the larger system and while there is still plenty more to learn I now have a foundation of understanding about wind energy and its beautiful power generating machines.

There were many moments during this research where I stumbled upon a neat fact or unique underlying theory that I felt compelled to share but couldn't find a way to integrate it into this paper. This research is definitely not the sum of all that I have learned in the past few months, and I am glad to have had the opportunity to pursue my interest in renewable energy. "The future is green energy, sustainability, renewable energy" – Arnold Schwarzenegger.

CHAPTER 8: REFERENCES

- Aarhus. (2017, June 6). *The world's most powerful available wind turbine gets major power boost*. Retrieved from MHI Vestas Offshore Wind: <http://www.mhivestasoffshore.com/worlds-most-powerful-available-wind-turbine-gets-major-power-boost/>
- Ahmed, M. G. (2016). *Utilization of Wind Energy in Green Buildings*. Conference Paper, Zagazig University, Egypt, Department of Mechanical Engineering.
- American Wind Energy Association. (2017). *U.S. Wind Industry Fourth Quarter 2017 Market Report*.
- Ashuri, T. e. (2016). *Multidisciplinary design optimization of large wind turbines— Technical, Economic, and design challenges*. Elsevier.
- Attar, A. G. (2012). *Optimal Design of Lattice Wind Turbine Towers*. Conference Report.
- Big Stone Renewables Services. (n.d.). Retrieved April 2018, from Big Stone Renewables Web site: <https://bigstonerenewables.com/services/>
- Blackwood, M. (2016). *Maximum Efficiency of a Wind Turbine*. University of South Florida. Ungergraduate Journal of Mathematical Modeling: One + Two.
- Bulder, B. e. (2012). *Upscaling Wind Turbines*. Aalborg University Denmark.
- Carillo, C. (2014). *An Approach to Determine the Weibull Parameters for Wind Energy Analysis: The Case of Galicia (Spain)*. Multidisciplinary Digital Publishing Institute - Energies.
- Clifton, A., & Wagner, R. (2014). *Accounting for the effect of turbulence on wind turbine power curves*. Journal of Physics.
- Corcadden, K. e. (2016). *The Impact of Variable Wind Shear Coefficients on Risk Reduction of Wind Energy Projects*. National Center for Biotechnology Information.
- Distributed Wind Energy Association. (2014). *Tower Height*. Briefing Paper.
- Engström, S. e. (2010). *Tall towers for large wind turbines*. Project Report, Elforsk.
- Federal Aviation Administration. (2018, April 2). *Wind Turbine FAQs*. Retrieved April 9, 2018, from Obstruction Evaluation / Airport Airspace Analysis Web site: <https://oeaaa.faa.gov/oeaaa/external/searchAction.jsp?action=showWindTurbineFAQs>

Florez, J. (2015, November 4). *Acciona Windpower reaches 1,000 MW of wind turbines installed with concrete towers*. Retrieved April 2018, from Santamarta Florez Blogspot: <http://santamarta-florez.blogspot.com/2015/11/acciona-windpower-reaches-1000-mw-of.html>

GE Renewable Energy. (n.d.). *About the 2.75-120 Wind Turbine*. Retrieved April 2018, from <https://www.gerenewableenergy.com/wind-energy/turbines/275-120>

Global Wind Energy Council. (2017). *Global Wind Statistics 2017*.

Hedevang, E. (2014). *Wind turbine power curves incorporating turbulence intensity*. Wind Energy.

Homer Energy. (n.d.). *Weibull k Value*. Retrieved April 2018, from https://www.homerenergy.com/products/pro/docs/3.11/weibull_k_value.html

International Energy Agency. (2017). *Renewables 2017*.

International Renewable Energy Agency. (2012). *Renewable Energy Technologies: Cost Analysis Series*.

Jimeno, J. (n.d.). *Concrete Towers for Multi-Megawatt Turbines*. Retrieved April 2018, from Wind Systems Web site: <http://www.windsystemsmag.com/article/detail/334/concrete-towers-for-multi-megawatt-turbines>

Kellner, T. (2018, March 1). *Making Waves: GE Unveils Plans To Build An Offshore Wind Turbine The Size Of A Skyscraper, The World's Most Powerful*. Retrieved April 2018, from GE Reports: <https://www.ge.com/reports/making-waves-ge-unveils-plans-build-offshore-wind-turbine-size-skyscraper-worlds-powerful/>

Larson, G., & Hansen, K. (2001). *Database on Wind Characteristics*. Riso National Laboratory Roskilde.

Lundquist, J., & Clifton, A. (2012, September). *How turbulence can impact power performance*. Retrieved April 2018, from National Wind Watch: <https://www.wind-watch.org/documents/how-turbulence-can-impact-power-performance/>

Miceli, F. (2012, April 30). *Patrick Henderson foundation*. Retrieved April 2018, from Wind Farm Bop Website: <http://www.windfarmbop.com/patrick-henderson-foundation/>

National Renewable Energy Laboratory. (2000). *WindPACT Turbine Design Scaling Studies Technical Area 2: Turbine, Rotor, and Blade Logistics*. Subcontractor Report, National Renewable Energy Laboratory, Kirkland, Washington.

- National Renewable Energy Laboratory. (2006). *Wind Turbine Design Cost and Scaling Model*. Technical Report.
- National Renewable Energy Laboratory. (n.d.). *Oklahoma 30-Meter Residential-Scale Wind Resource Map*. Retrieved April 2018, from Wind Exchange Web site:
<https://windexchange.energy.gov/maps-data/300>
- National Renewable Energy Laboratory. (n.d.). *Wyoming 30-Meter Residential-Scale Wind Resource Map*. Retrieved April 2018, from Wind Exchange Web site:
<https://windexchange.energy.gov/maps-data/318>
- National Renewable Energy Laboratory. (2001). *WindPACT Turbine Design Scaling Studies: Technical Area 4 - Balance of Station Cost*. US Department of Energy. Jackson, Michigan: Commonwealth Associates, Inc.
- National Water & Climate Center. (2002, June). *Index of Windrose*. Retrieved April 2018, from
<https://www.wcc.nrcs.usda.gov/ftpref/downloads/climate/windrose/>
- Nicholson, J. (2011). *Design of wind turbine tower and foundation systems: optimization approach*. Masters Thesis, Iowa University.
- Nielsen, M. (2011). *Parameter Estimation for the Two-Parameter Weibull Distribution*. Master's Thesis, Brigham Young University, Department of Statistics.
- Ozturk, F. (2016). *Finite Element Modeling of Tubular Bolted Connection of a Lattice Wind Tower For Fatigue Assessment*. Masters Thesis, University of Coimbra.
- PacifiCorp. (2011, November 11). *Seven Mile Hill Wind Project*. Retrieved April 2018, from PacifiCorp Web site:
http://www.pacificorp.com/content/dam/pacificorp/doc/Energy_Sources/EnergyGeneration_FactSheets/RMP_GFS_Seven_Mile_Hill.pdf
- Ray, M. L., Rogers, A. L., & McGowan, J. G. (2006). *Analysis of wind shear models and trends in different terrains*. Renewable Energy Research Laboratory.
- REN21. (2017). *Renewables 2017 Global Status Report*.

- Schaefer, V. A. (2011). *Foundations for Wind Turbines*. Retrieved April 2018, from <http://home.eng.iastate.edu/~jdm/engr340-2011/ENGR%20340%20-%20Foundations%203%20-%20Ashlock%20-%20Schaefer.pdf>
- Schmidt, M. (2007). *The Economic Optimization of Wind Turbine Design*. Masters Thesis, Georgia Institute of Technology, Department of Mechanical Engineering.
- Shahan, Z. (2016, December 26). *Low Costs of Solar Power & Wind Power Crush Coal, Crush Nuclear, and Beat Natural Gas*. Retrieved April 2018, from Clean Technica: <https://cleantechnica.com/2016/12/25/cost-of-solar-power-vs-cost-of-wind-power-coal-nuclear-natural-gas/>
- Standardized Extreme Wind Speed Database for the United States. (2016). National Institute of Standards and Technology. Retrieved April 2018, from https://www.itl.nist.gov/div898/winds/NIST_TN/nist_tn.htm
- Tackle TW 1.5S*. (n.d.). Retrieved April 2018, from Wind Turbine Models Web site: <https://www.en.wind-turbine-models.com/turbines/27-tacke-tw-1.5s>
- Tchakoua P., e. a. (2013). *A Review of Concepts and Methods for Wind Turbines Condition Monitoring*. Conference Paper.
- Tensionless Pier Wind Turbine Foundation*. (n.d.). Retrieved April 2018, from Contech Engineered Solutions Web site: <http://www.conteches.com/Markets/Wind-Turbine-Foundations/Tensionless-Pier-Wind-Turbine-Foundation>
- The Wind Power. (n.d.). *Power Curves Database*. Retrieved April 2018, from https://www.thewindpower.net/store_manufacturer_turbine_en.php?id_type=7
- U.S. Department of Energy. (n.d.). *Levelized Cost of Energy*. Retrieved April 2018, from Energy.gov Web site: <https://www.energy.gov/sites/prod/files/2015/08/f25/LCOE.pdf>
- United States Geological Survey. (2016). *Onshore Industrial Wind Turbine Locations for the United States to March 2014*. Online Database, United States Geological Survey.
- US Department of Energy. (n.d.). *The Inside of a Wind Turbine*. Retrieved from Energy.Gov: <https://www.energy.gov/eere/wind/inside-wind-turbine-0>
- US Energy Information Administration. (2018). *Annual Energy Outlook 2018*. Washington D.C. .

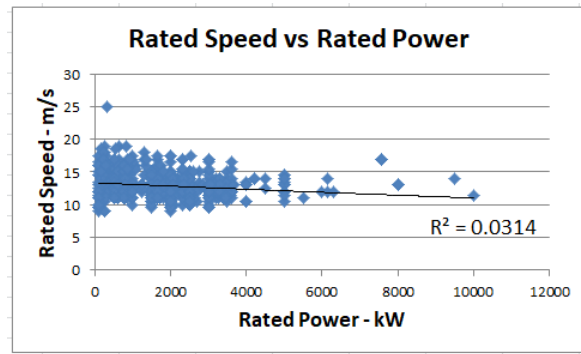
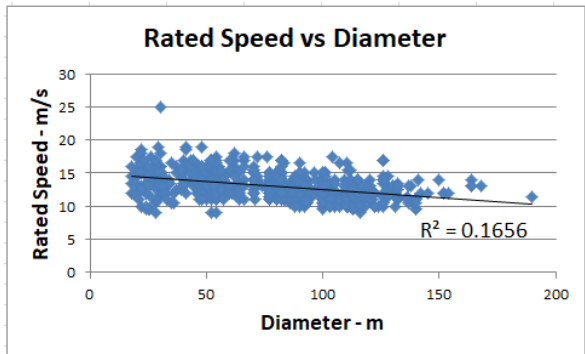
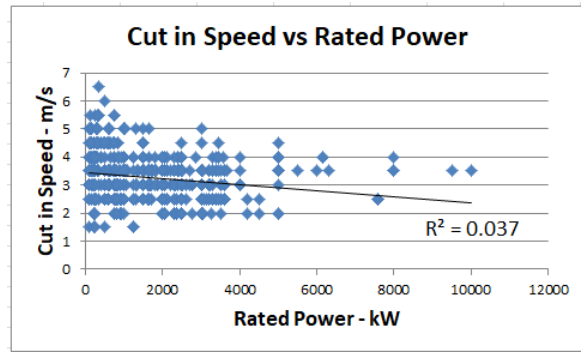
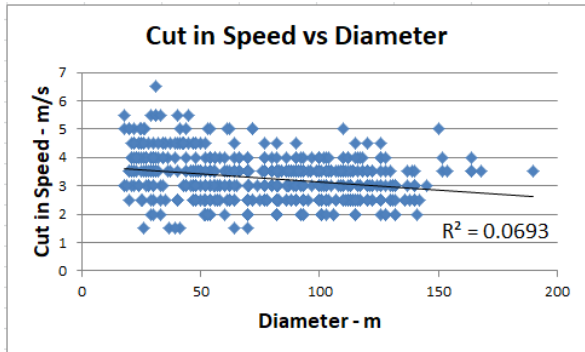
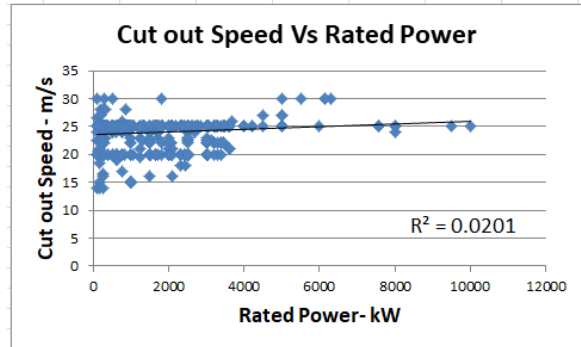
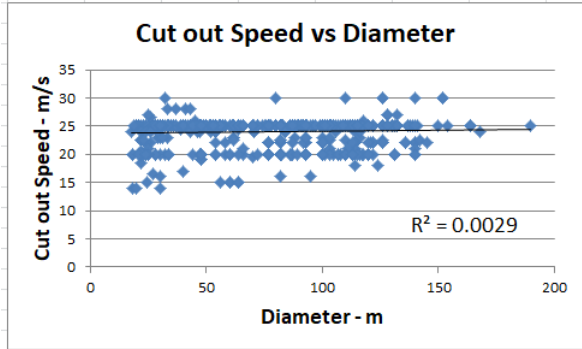
Wan, Y., Ela, E., & Orwig, K. (2010). *Development of an Equivalent Wind Plant Power Curve*. Dallas, TX: National Renewable Energy Laboratory.

Wind Energy Foundation. (n.d.). *History of Wind Energy*. Retrieved April 2018, from <http://windenergyfoundation.org/about-wind-energy/history/>

World Nuclear Association. (2018, January). *Outline History of Nuclear Energy*. Retrieved 2018 April, from <http://www.world-nuclear.org/information-library/current-and-future-generation/outline-history-of-nuclear-energy.aspx>

CHAPTER 9: APPENDIX

APPENDIX A – Cut in, Cut out, and Rated Speed relationships



APPENDIX B - Power Curve Trendline Data

d	a	b	R ²	d	a	b	R ²	d	a	b	R ²	d	a	b	R ²
30	0.140	2.910	0.956	73	0.769	3.085	0.976	116	2.085	3.107	0.989	159	1.464	3.506	0.962
31	0.159	2.978	0.977	74	0.708	3.168	0.985	117	2.065	3.091	0.981	160	1.480	3.510	0.964
32	0.084	3.356	0.990	75	0.583	3.249	0.997	118	1.577	3.244	0.980	161	1.495	3.515	0.967
33	0.545	2.581	0.988	76	1.940	2.633	0.926	119	2.745	2.972	0.976	162	1.510	3.519	0.969
34	0.151	3.230	0.933	77	0.753	3.147	0.980	120	3.885	2.812	0.974	163	1.801	3.429	0.965
35	0.343	2.794	0.973	78	1.221	2.985	0.992	121	5.123	2.709	0.980	164	1.812	3.434	0.967
36	0.129	3.178	0.996	79	1.152	3.010	0.983	122	2.755	3.007	0.982	165	1.675	3.463	0.961
37	0.297	2.781	0.987	80	1.083	3.035	0.972	123	2.645	3.026	0.978	166	1.527	3.497	0.954
38	0.098	3.376	0.874	81	1.426	2.907	0.968	124	1.973	3.199	0.982	167	1.149	3.637	0.950
39	0.426	2.908	0.738	82	1.608	2.864	0.970	125	4.735	2.754	0.977	168	1.000	3.692	0.940
40	0.239	3.048	0.978	83	1.501	2.922	0.975	126	6.657	2.622	0.983	169	1.124	3.650	0.941
41	0.073	3.425	0.809	84	1.242	3.053	0.989	127	5.751	2.724	0.988	170	1.253	3.612	0.943
42	0.033	3.851	0.859	85	1.286	3.032	0.982	128	4.950	2.828	0.992	171	1.386	3.576	0.944
43	0.374	2.904	0.967	86	1.162	3.088	0.979	129	4.388	2.854	0.985	172	1.282	3.642	0.950
44	0.336	2.976	0.958	87	1.929	2.840	0.975	130	3.772	2.893	0.972	173	1.400	3.612	0.951
45	0.009	4.546	0.916	88	0.580	3.393	0.983	131	4.371	2.839	0.972	174	1.522	3.584	0.952
46	0.274	3.071	0.976	89	1.806	2.876	0.979	132	12.972	2.384	0.978	175	1.646	3.558	0.953
47	0.794	2.684	0.965	90	1.411	3.018	0.980	133	10.986	2.451	0.974	176	1.773	3.533	0.954
48	0.443	2.933	0.973	91	1.440	3.074	0.993	134	9.140	2.525	0.971	177	1.902	3.511	0.955
49	0.837	2.658	0.969	92	1.124	3.150	0.979	135	6.332	2.703	0.975	178	2.034	3.489	0.956
50	0.393	3.001	0.971	93	1.934	2.919	0.977	136	4.938	2.808	0.971	179	2.168	3.469	0.956
51	0.832	2.686	0.966	94	5.657	2.497	0.987	137	4.950	2.815	0.973	180	1.937	3.550	0.962
52	1.321	2.512	0.964	95	12.265	2.187	0.985	138	8.661	2.503	0.952	181	2.052	3.532	0.962
53	0.967	2.699	0.978	96	1.344	3.068	0.967	139	0.598	3.933	0.983	182	2.169	3.515	0.963
54	0.799	2.775	0.956	97	1.611	2.959	0.930	140	3.173	3.087	0.988	183	2.287	3.499	0.964
55	0.812	2.827	0.971	98	1.624	2.986	0.955	141	10.149	2.447	0.948	184	2.407	3.484	0.964
56	0.775	2.909	0.984	99	1.900	2.925	0.966	142	9.135	2.522	0.946	185	2.528	3.469	0.965
57	0.842	2.863	0.991	100	1.533	3.091	0.976	143	5.694	2.705	0.958	186	2.650	3.456	0.965
58	0.561	2.999	0.974	101	4.065	2.647	0.981	144	3.129	2.941	0.967	187	2.339	3.542	0.970
59	0.805	2.871	0.976	102	0.933	3.335	0.976	145	1.390	3.267	0.972	188	2.444	3.529	0.971
60	1.081	2.770	0.978	103	2.626	2.905	0.985	146	1.305	3.349	0.974	189	2.550	3.517	0.971
61	1.432	2.650	0.968	104	1.852	3.029	0.966	147	1.240	3.419	0.975	190	2.656	3.506	0.971
62	0.857	2.881	0.968	105	1.239	3.201	0.984	148	1.190	3.481	0.975	191	2.763	3.495	0.972
63	0.853	2.908	0.972	106	8.467	2.375	0.987	149	1.149	3.536	0.975	192	2.871	3.485	0.972
64	0.727	3.021	0.983	107	2.751	2.873	0.971	150	1.116	3.585	0.975	193	2.980	3.475	0.973
65	0.254	3.508	0.990	108	0.911	3.411	0.977	151	1.088	3.630	0.974	194	2.661	3.553	0.976
66	1.302	2.760	0.958	109	2.855	2.850	0.975	152	1.065	3.670	0.973	195	2.758	3.543	0.976
67	1.128	2.851	0.967	110	1.999	3.005	0.981	153	1.001	3.688	0.968	196	2.856	3.534	0.976
68	1.105	2.874	0.970	111	3.007	2.801	0.969	154	0.923	3.715	0.961	197	2.954	3.525	0.977
69	0.953	2.967	0.977	112	2.072	3.013	0.981	155	0.947	3.712	0.964	198	3.052	3.517	0.977
70	0.824	3.059	0.983	113	2.897	2.924	0.990	156	1.169	3.602	0.961	199	3.151	3.508	0.977
71	0.239	3.600	0.991	114	2.581	2.961	0.982	157	1.189	3.604	0.963	200	3.251	3.500	0.977

APPENDIX C - INITIAL CAPITAL COST BREAKDOWN

The scaling equations used in this simulation are taken directly from the Wind Pact Design Cost and Scaling Model but are restated here.

Blade Mass – Based on advanced material	$0.4948r^{2.53}$
Blade Cost – Cost is for a single blade	$0.5582r^3 + 3.8118r^{2.5025} - 955.24$
Hub Mass	$0.954 * Blade_Mass + 5680.3$
Hub Cost	$4.25 * Hub_Mass$
Pitch Bearing Mechanism Cost	$2.28 * (0.2106 * d^{2.6578})$
Nose Cone Mass	$18.5d - 520.5$
Nose Cone Cost	$5.57 * Nose_Cone_Mass$
Low Speed Shaft Cost	$0.1d^{2.887}$
Bearing Mass	$(\frac{8d}{600} - 0.033) * 0.0092d^{2.5}$
Bearing Cost	$2 * Bearing_Mass * 17.6$
Gearbox Cost – Based on three-stage Planetary/ Helical gearbox	$16.45PR^{1.249}$
Brake Cost	$1.9894PR - 0.1141$
Generator Cost – Three stage drive with high speed generator	$65 * PR$
Variable Speed Electronics Cost	$79 * PR$
Yaw Drive Cost	$2 * (0.0339d^{2.964})$
Mainframe Mass	$2.233d^{1.953}$
Mainframe Cost	$9.489 * 3 * d^{1.953}$
Platforms Railings Mass	$0.125 * Mainframe_Mass$
Platforms Railings Cost	$8.7 * Platforms_Railings_Mass$
Electrical Connection Cost	$40 * PR$
Hydraulic Cooling Cost	$12 * PR$
Nacelle Cover Cost	$11.537 * PR + 3849.7$
Control Safety Monitoring Cost	35000
Tower Mass	$0.3973 * A * h - 1414$
Tower Cost	$Tower_Mass * 1.5$
Foundation Cost	$303.24 * (h * A)^{0.4037}$
Transportation Cost	$(1.581 * 10^{-5}) * PR^3 - 0.0375PR^2 + 54.7PR$

Roads Civil Cost	$[(2.17 * 10^{-6}) * PR^2 - 0.0145 * PR + 69.54] * PR$
Assembly and Installation Cost	$1.965(h * d)^{1.1736}$
Electrical Interface Cost	$[(3.49 * 10^{-6}) * PR^2 - 0.0221PR + 109.7] * PR$
Engineering and Permits Cost	$[(9.94 * 10^{-4}) * PR + 20.31] * PR$
Initial Capital Cost	Blades Cost * 3 + Hub Cost + Pitch Bearing Mechanism Cost + Nose Cone Cost + Low Speed Shaft Cost + Bearing Cost + Gearbox Cost + Brake Cost + Generator Cost + Variable Speed Electronics Cost + Yaw Drive Cost + Mainframe Cost + Platforms Railings Cost + Electrical Connection Cost + Hydraulic Cooling Cost + Nacelle Cover Cost + Control Safety Monitoring Cost + Tower Cost + Foundation Cost + Transportation Cost + Roads Civil Cost + Assembly and Installation Cost + Electrical Interface Cost + Engineering Permits Cost

APPENDIX D – COE/LF SIMULATION FLOWCHART

